Adaptive time-frequency detection and filtering for imaging in strongly heterogeneous background media

Chrysoula Tsogka

tsogka@tem.uoc.gr

http://tem.uoc.gr/˜tsogka

University of Crete & IACM-FORTH

In Collaboration with:

Liliana Borcea (Rice University)

George Papanicolaou (Stanford University)

Support: EU: MIRG-CT-2007-203438, ERC-STG: 239959

Imaging in heavy clutter

Problem: Image compactly supported reflectors buried in heterogeneous, strongly backscattering media, using an array of sensors.

Difficulty: The echoes from the reflector are overwhelmed by the backscattered field from the background medium.

Idea: Filter the data prior to imaging so as to remove the unwanted backscattered field.

Imaging in heavy clutter

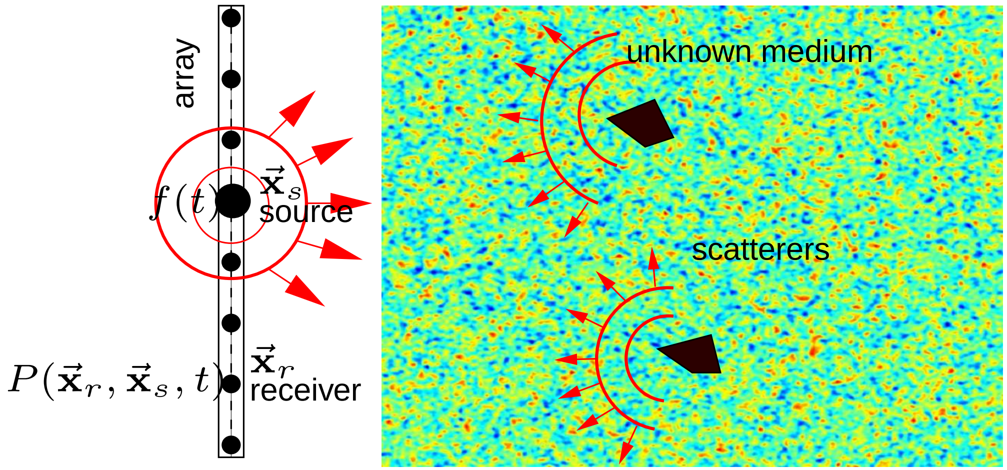

Propagation medium: heterogeneous, strongly backscattering medium

Data: Acoustic pressure $P(\vec{\mathbf{x}}_r, \vec{\mathbf{x}}_s, t)$ for $(\vec{\mathbf{x}}_s, \vec{\mathbf{x}}_r)$ a set of source and receiver locations on the array.

Reflector: scatterer with compact support

Imaging in heavy clutter

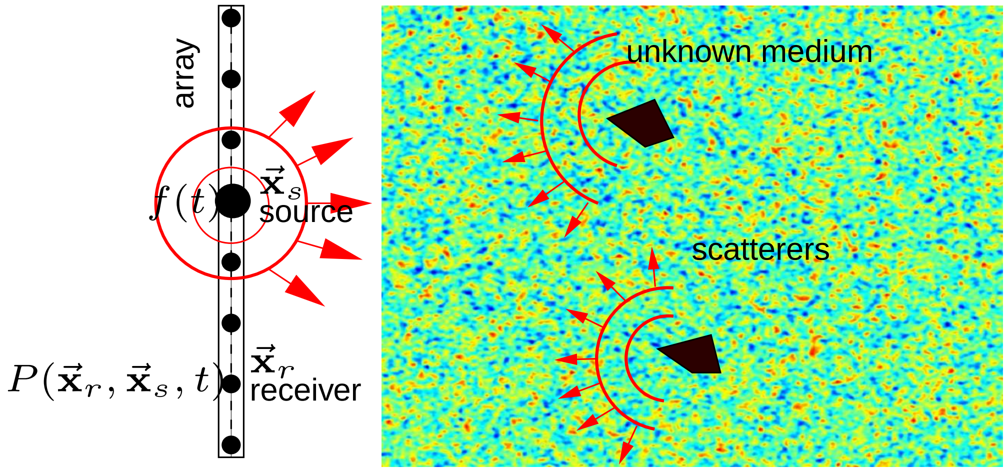

Model: P satisfies the acoustic wave eq. with velocity $v(\vec{\mathbf{x}})$

$$\frac{1}{v^2(\vec{\mathbf{x}})} = \frac{1}{c^2(\vec{\mathbf{x}})}\left[1 + \sigma\mu\left(\frac{x}{\ell_x}, \frac{z}{\ell_z}\right) + \nu(\vec{\mathbf{x}})\right],$$

we know or can determine the smooth $c(\vec{\mathbf{x}})$ and we model the fluctuations with mean zero random, stationary process μ

ℓ_x, ℓ_z: correlation lengths and σ gives strength of fluctuations.

Imaging in heavy clutter

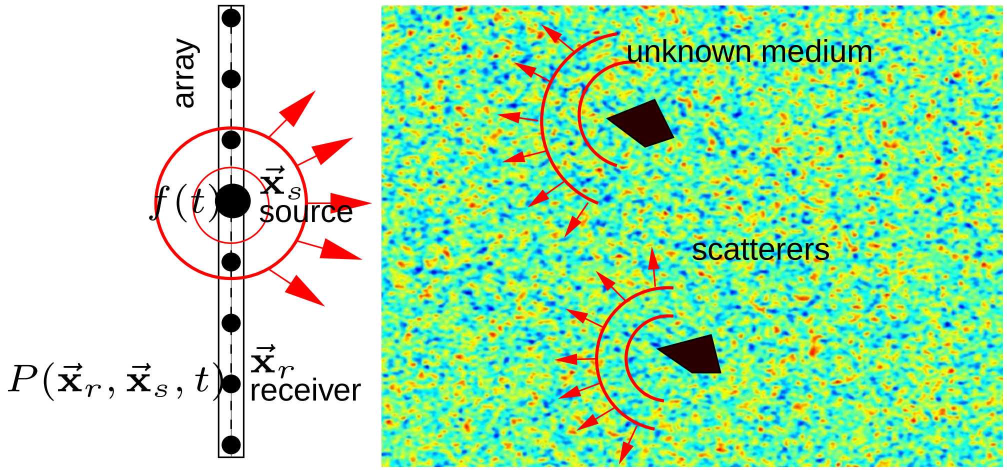

Model: P satisfies the acoustic wave eq. with velocity $v(\vec{\mathbf{x}})$

$$\frac{1}{v^2(\vec{\mathbf{x}})} = \frac{1}{c^2(\vec{\mathbf{x}})}\left[1 + \sigma\mu\left(\frac{x}{\ell_x}, \frac{z}{\ell_z}\right) + \nu(\vec{\mathbf{x}})\right],$$

$\nu(\vec{\mathbf{x}})$ is the reflectivity of the scatterer to be imaged.

Velocity profile in the earth

- background velocity consists of a smooth part $c(\vec{\mathbf{x}})$ (assumed known), and of the fluctuations, which cannot be estimated.

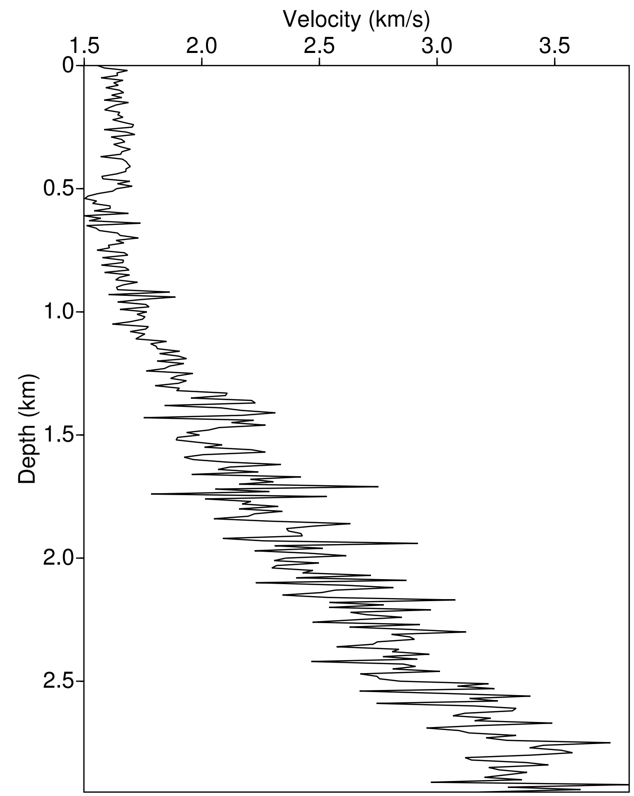

- Velocity profile in a well log

Synthetic realization of random media

isotropic

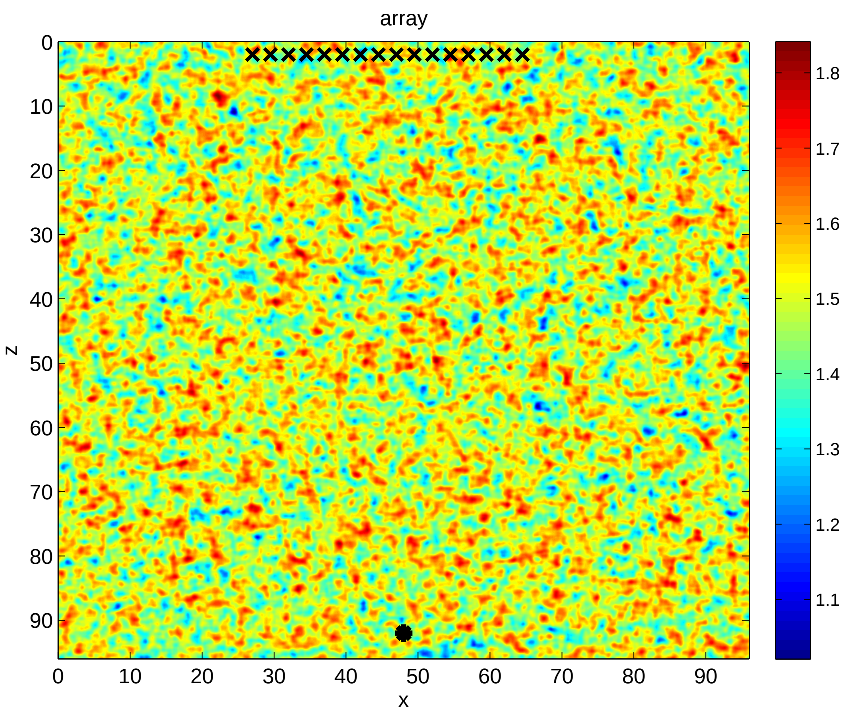

layered

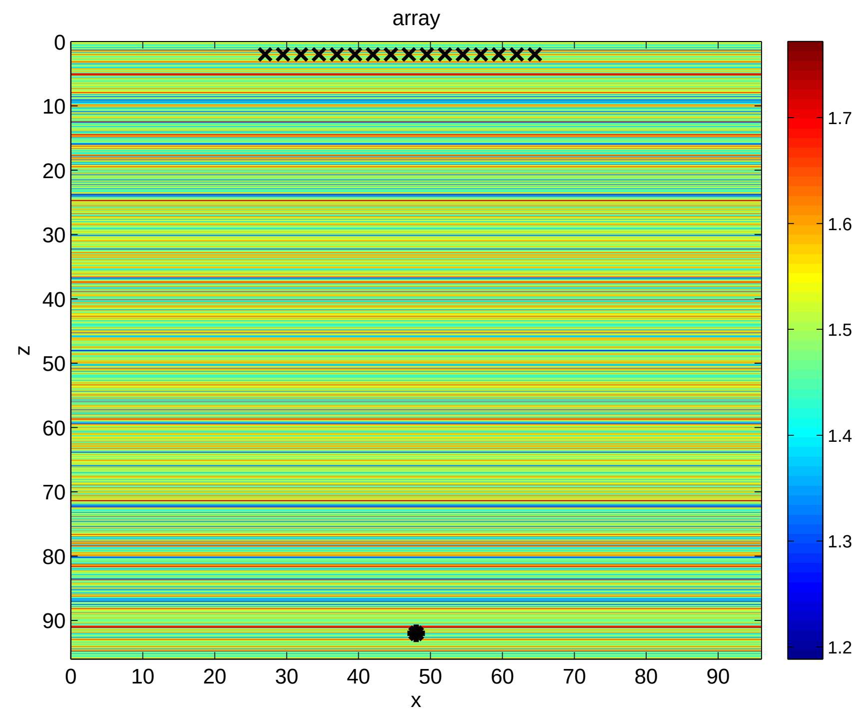

- in both cases $c(\vec{\mathbf{x}}) = c_0 = 1.5$km/s
- isotropic $\ell_x = \ell_z = \ell = \lambda_0/4$, $\sigma = 0.12$
- layered $\ell_x = \infty$, $\ell_z = \lambda_0/50$, $\sigma = 0.08$

Synthetic realization of random media

isotropic

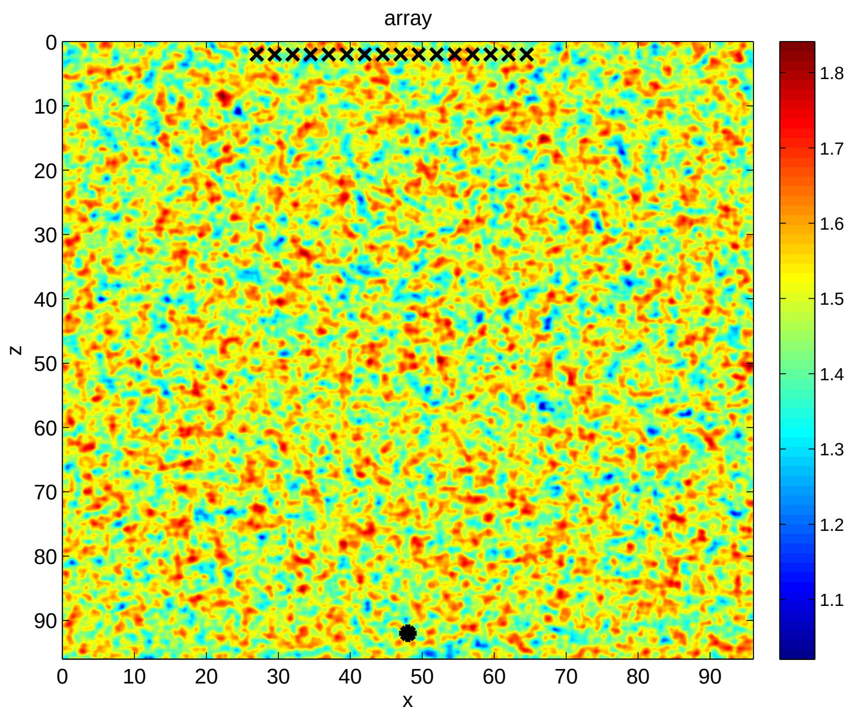

layered

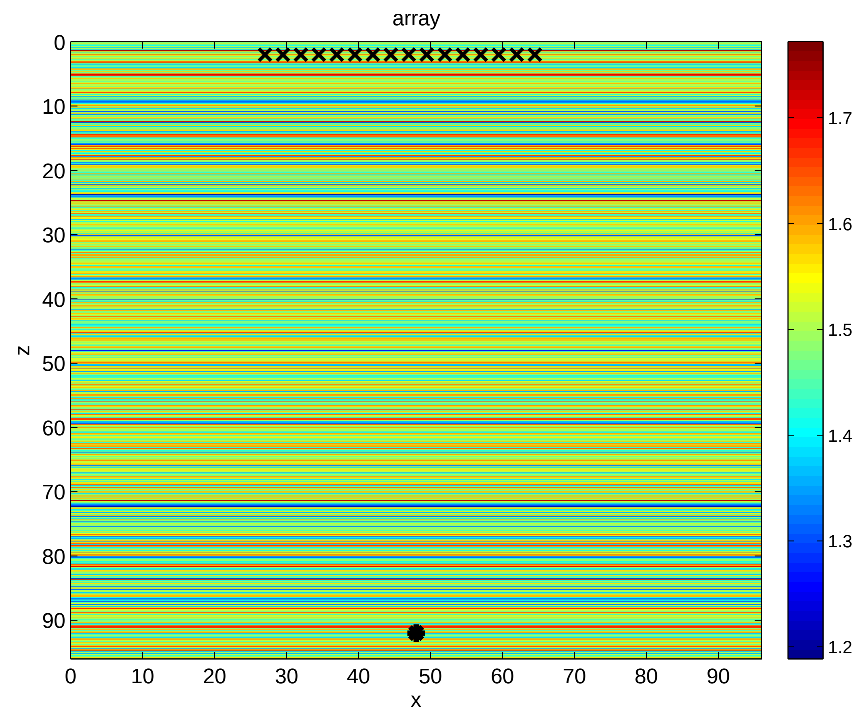

- Correlation function (isotropic)

$$E\{\mu_i(\vec{\mathbf{x}}_1)\mu_i(\vec{\mathbf{x}}_2)\} = R(\vec{\mathbf{x}}_1, \vec{\mathbf{x}}_2) = \left(1 + \frac{|\vec{\mathbf{x}}_1 - \vec{\mathbf{x}}_2|}{\ell}\right) e^{-\frac{|\vec{\mathbf{x}}_1 - \vec{\mathbf{x}}_2|}{\ell}}$$

Synthetic realization of random media

isotropic

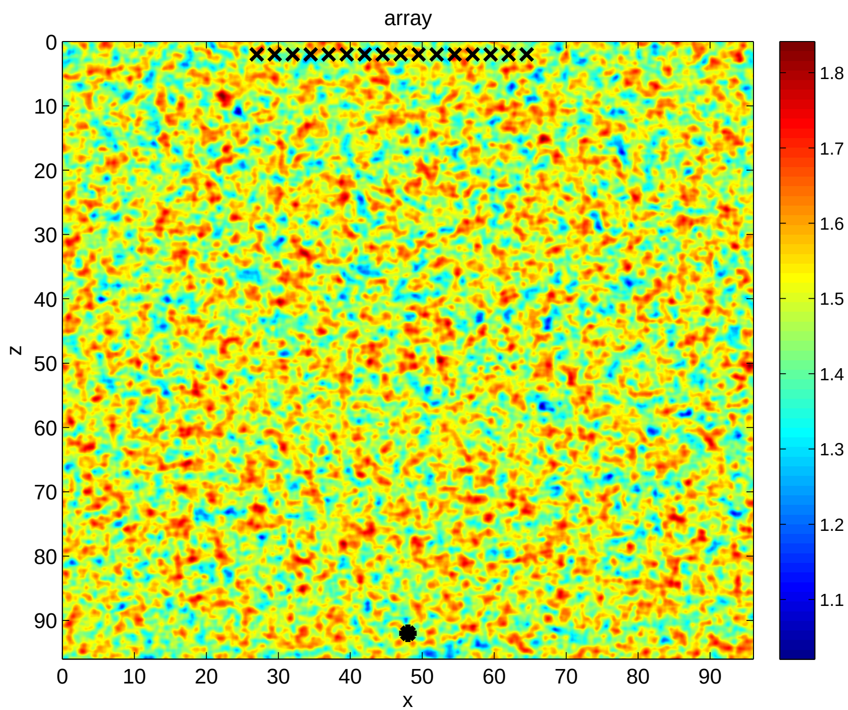

layered

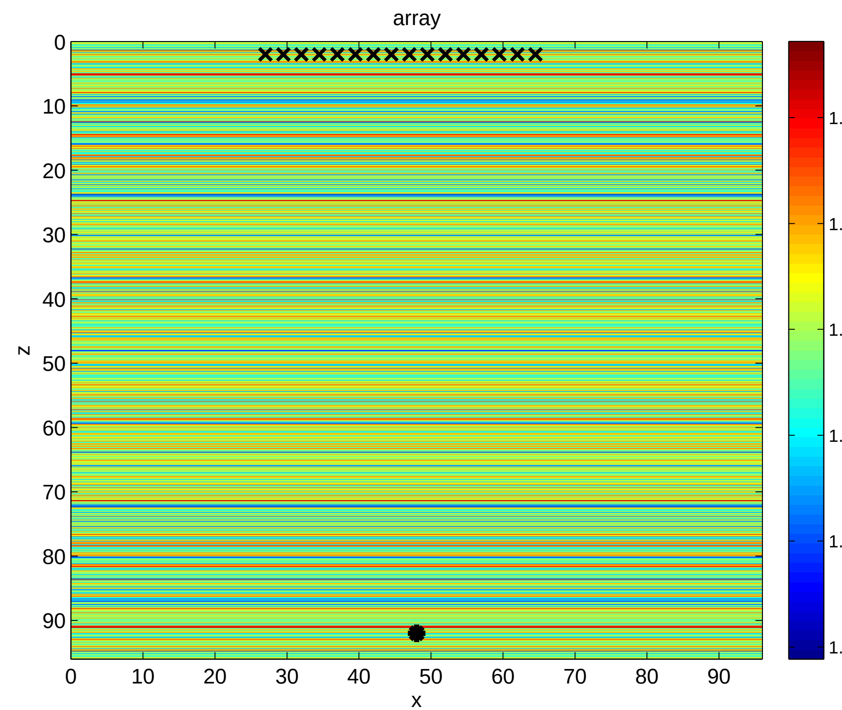

- Correlation function (layered)

$$E\{\mu_l(z_1)\mu_l(z_2)\} = \left(1 + \frac{|z_1 - z_2|}{\ell_z}\right) e^{-\frac{|z_1 - z_2|}{\ell_z}}$$

The imaging problem

- recover the support of $\nu(\vec{\mathbf{x}})$ from $P(\vec{\mathbf{x}}_r, \vec{\mathbf{x}}_s, t)$

  $P(\vec{\mathbf{x}}_r, \vec{\mathbf{x}}_s, t) \xrightarrow{\text{Fourier}} \hat{P}(\vec{\mathbf{x}}_r, \vec{\mathbf{x}}_s, \omega)$ in some frequency range $\omega \in [\omega_0 - B/2, \omega_0 + B/2]$.

- The solution of the linearized least squares problem:

$$J(\nu) = \int d\omega \sum_{\vec{\mathbf{x}}_r, \vec{\mathbf{x}}_s} |\hat{P}(\vec{\mathbf{x}}_r, \vec{\mathbf{x}}_s, \omega) - \hat{Q}_L(\vec{\mathbf{x}}_r, \vec{\mathbf{x}}_s, \omega; \nu)|^2$$

- with (linearized model) $Q_L(\vec{\mathbf{x}}_r, \vec{\mathbf{x}}_s, \omega; \nu) = \mathcal{A}\,\nu$

$$\hat{Q}_L(\vec{\mathbf{x}}_r, \vec{\mathbf{x}}_s, \omega; \nu) = -k^2 \hat{f}(\omega) \int \nu(\vec{\mathbf{z}}) \widehat{G}_{BG}(\vec{\mathbf{x}}_s, \vec{\mathbf{z}}, \omega) \widehat{G}_{BG}(\vec{\mathbf{z}}, \vec{\mathbf{x}}_r, \omega) d\vec{\mathbf{z}}$$

- is given by $\nu_{LSQ} = (\mathcal{A}^H \mathcal{A})^{-1} \mathcal{A}^H \hat{P}(\vec{\mathbf{x}}_r, \vec{\mathbf{x}}_s, \omega)$.

The imaging problem

- recover the support of $\nu(\vec{\mathbf{x}})$ from $P(\vec{\mathbf{x}}_r, \vec{\mathbf{x}}_s, t)$

  $P(\vec{\mathbf{x}}_r, \vec{\mathbf{x}}_s, t) \xrightarrow{\text{Fourier}} \hat{P}(\vec{\mathbf{x}}_r, \vec{\mathbf{x}}_s, \omega)$ in some frequency range $\omega \in [\omega_0 - B/2, \omega_0 + B/2]$.

- Approximating $\mathcal{A}^H \mathcal{A}$ by the identity operator gives

$$\begin{aligned} \nu_{IM}(\vec{\mathbf{z}}) &= \mathcal{A}^H \hat{P}(\vec{\mathbf{x}}_r, \vec{\mathbf{x}}_s, \omega) \\ &= \int d\omega k^2 \hat{f}(\omega) \sum_{\vec{\mathbf{x}}_s, \vec{\mathbf{x}}_r} \hat{P}(\vec{\mathbf{x}}_r, \vec{\mathbf{x}}_s, \omega) \overline{\widehat{G}_{BG}(\vec{\mathbf{z}}, \vec{\mathbf{x}}_r, \omega) \widehat{G}_{BG}(\vec{\mathbf{x}}_s, \vec{\mathbf{z}}, \omega)} \end{aligned}$$

The imaging problem

- recover the support of $\nu(\vec{\mathbf{x}})$ from $P(\vec{\mathbf{x}}_r, \vec{\mathbf{x}}_s, t)$

  $P(\vec{\mathbf{x}}_r, \vec{\mathbf{x}}_s, t) \xrightarrow{\text{Fourier}} \hat{P}(\vec{\mathbf{x}}_r, \vec{\mathbf{x}}_s, \omega)$ in some frequency range $\omega \in [\omega_0 - B/2, \omega_0 + B/2]$.

- Migration method (ideally)

$$\mathcal{I}(\vec{\mathbf{y}}^s) = \int d\omega k^2 \hat{f}(\omega) \sum_{\vec{\mathbf{x}}_s, \vec{\mathbf{x}}_r} \hat{P}(\vec{\mathbf{x}}_r, \vec{\mathbf{x}}_s, \omega) \overline{\widehat{G}_{BG}(\vec{\mathbf{x}}_s, \vec{\mathbf{y}}^s, \omega) \widehat{G}_{BG}(\vec{\mathbf{x}}_r, \vec{\mathbf{y}}^s, \omega)}$$

- Backpropagating only in the known smooth $c(\vec{\mathbf{x}})$

$$\widehat{G}_{BG} \rightsquigarrow \widehat{G}_c(\vec{\mathbf{x}}, \vec{\mathbf{y}}, \omega) = \frac{e^{i\omega\tau(\vec{\mathbf{x}}, \vec{\mathbf{y}})}}{4\pi \left|\vec{\mathbf{x}} - \vec{\mathbf{y}}\right|} \sim e^{i\omega\tau(\vec{\mathbf{x}}, \vec{\mathbf{y}})}$$

  and neglecting amplitudes we get Kirchhoff migration

Kirchhoff migration

$$\mathcal{J}^{\mathsf{KM}}(\vec{\mathbf{y}}^s) = \sum_{\vec{\mathbf{x}}_s, \vec{\mathbf{x}}_r} \int d\omega \hat{P}(\vec{\mathbf{x}}_r, \vec{\mathbf{x}}_s, \omega) e^{-i\omega(\tau(\vec{\mathbf{x}}_s, \vec{\mathbf{y}}^s) + \tau(\vec{\mathbf{y}}^s, \vec{\mathbf{x}}_r))}$$

$\tau(\vec{\mathbf{x}}, \vec{\mathbf{y}})$ is the travel time

$$\tau(\vec{\mathbf{x}}, \vec{\mathbf{y}}) = \min \int \frac{1}{c(X(s))} ds$$

where the minimum is over all paths X that start at $\vec{\mathbf{x}}$ and end at $\vec{\mathbf{y}}$. For $c = c_0$ =cste,

$$\tau(\vec{\mathbf{x}}, \vec{\mathbf{y}}) = \frac{|\vec{\mathbf{x}} - \vec{\mathbf{y}}|}{c_0}$$

Kirchhoff migration resolution

- when the array size a and the bandwidth $B \to \infty \Rightarrow$

$$\mathcal{I}^{\mathsf{KM}}(\vec{\mathbf{y}}^s) \approx \int_{\mathcal{D}} \delta(\vec{\mathbf{y}} - \vec{\mathbf{y}}^s)\nu(\vec{\mathbf{y}})d\vec{\mathbf{y}}$$

- for finite a and $B \Rightarrow$
  - range resolution (direction of propagation): $\sigma_{\mathsf{r}} = \dfrac{c_0}{B}$
  - cross-range resolution: $\sigma_{\mathsf{cr}} = \dfrac{\lambda_0 L}{a}$
- references:

  - N. Bleistein, J.K. Cohen, and J.W. Stockwell Jr., *Mathematics of multidimensional seismic imaging, migration, and inversion.* Springer, New York, 2001.
  - W. Symes. *Lecture notes in seismic imaging.* Mathematical Geophysics Summer School, Stanford, available at www.trip.caam.rice.edu, 1998.

Modeling the data

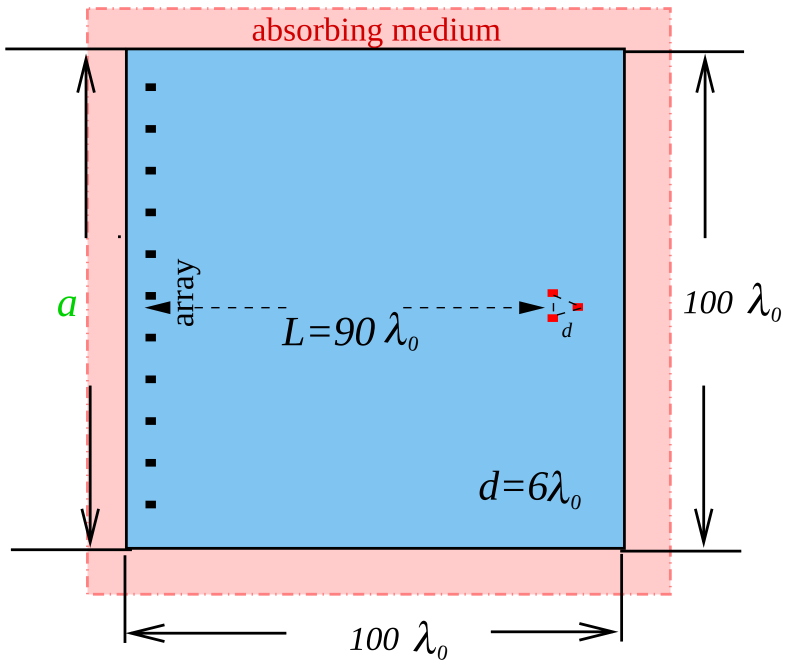

$$\varrho \frac{\partial \mathbf{v}}{\partial t} + \nabla P = 0$$

$$\frac{1}{\varrho v^2(\vec{\mathbf{x}})} \frac{\partial P}{\partial t} + \mathrm{div}\mathbf{v} = f(t)\delta(\vec{\mathbf{x}} - \vec{\mathbf{x}}_s)$$

- solve the 2d wave equation in a medium with velocity $v(\vec{\mathbf{x}})$ and cste density ϱ.
- unbounded domains are handled with the PML model.

Imaging results

The data

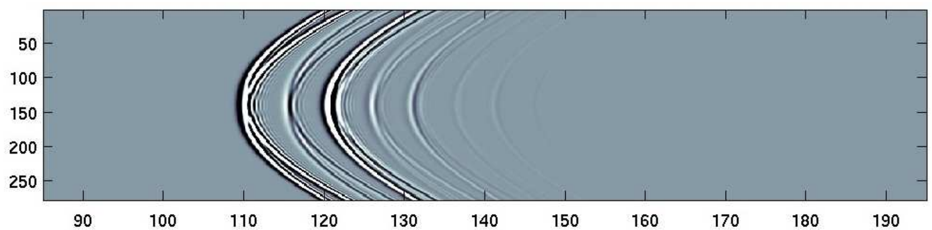

The image $\mathcal{J}^{\mathsf{KM}}(\vec{\mathbf{y}}^s)$

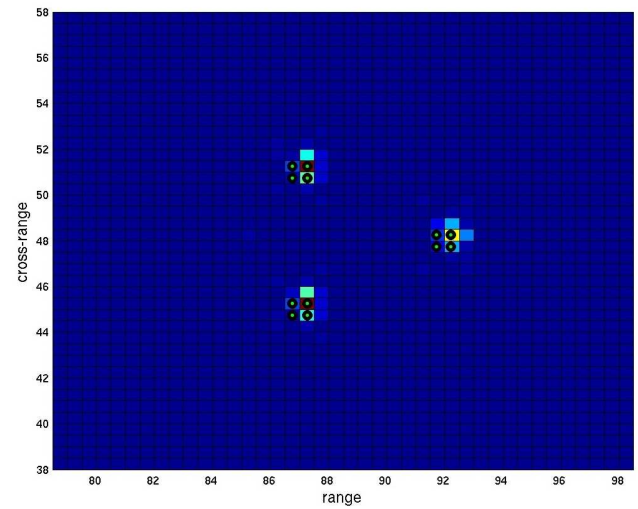

$$\mathcal{J}^{\mathsf{KM}}(\vec{\mathbf{y}}^s) = \sum_{\vec{\mathbf{x}}_s,\vec{\mathbf{x}}_r} \int d\omega \hat{P}(\vec{\mathbf{x}}_r, \vec{\mathbf{x}}_s, \omega) e^{-i\omega(\tau(\vec{\mathbf{x}}_s,\vec{\mathbf{y}}^s)+\tau(\vec{\mathbf{y}}^s,\vec{\mathbf{x}}_r))}$$

For $c(\vec{\mathbf{x}}) = c_0$ cst, $\tau(\vec{\mathbf{y}}, \vec{\mathbf{x}}) = \frac{|\vec{\mathbf{x}}-\vec{\mathbf{y}}|}{c_0}$

Note: we consider here a single source, the array center

What happens in clutter?

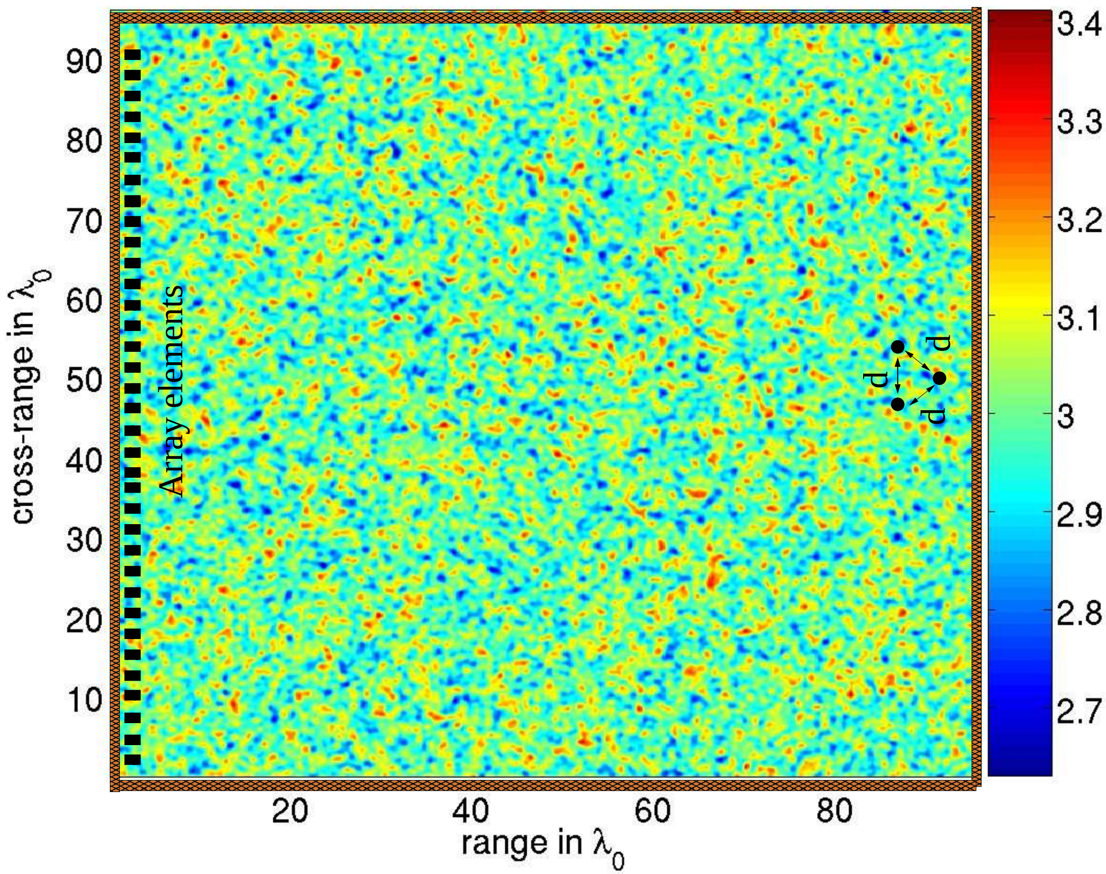

- Length scaled by λ_0, velocity in km/sec

What happens in clutter?

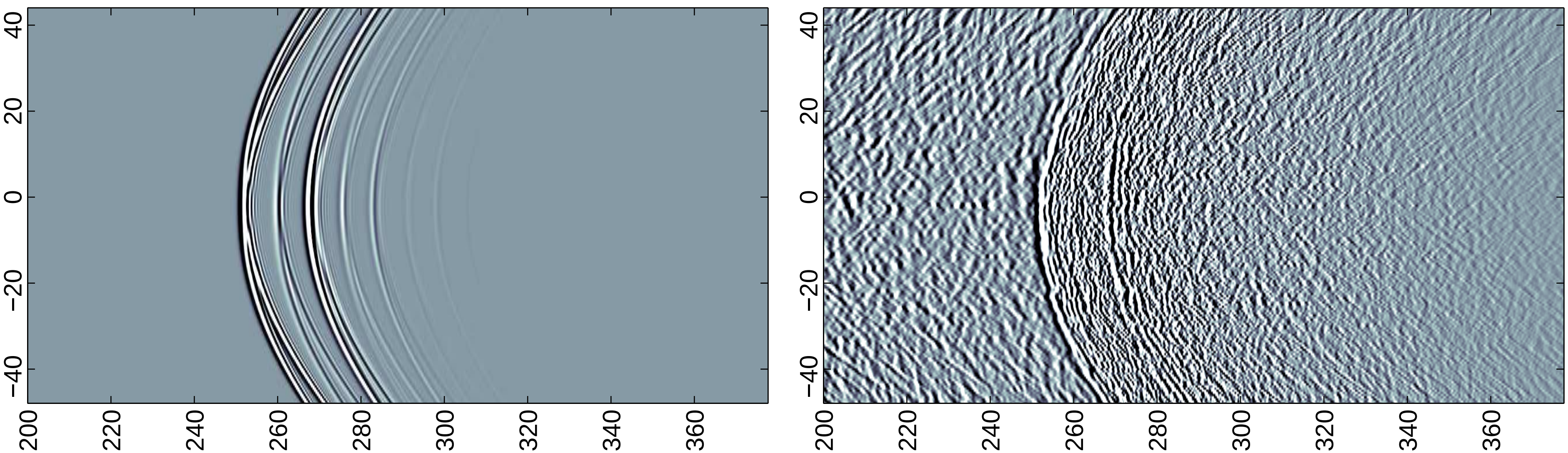

- Length scaled by λ_0 and time by pulsewidth
- the clutter impedes the imaging process as the significant multipathing of the waves by the inhomogeneities results to noisy data traces (the noise is not simply additive)

Migration in clutter

- Classic migration is statisticaly unstable

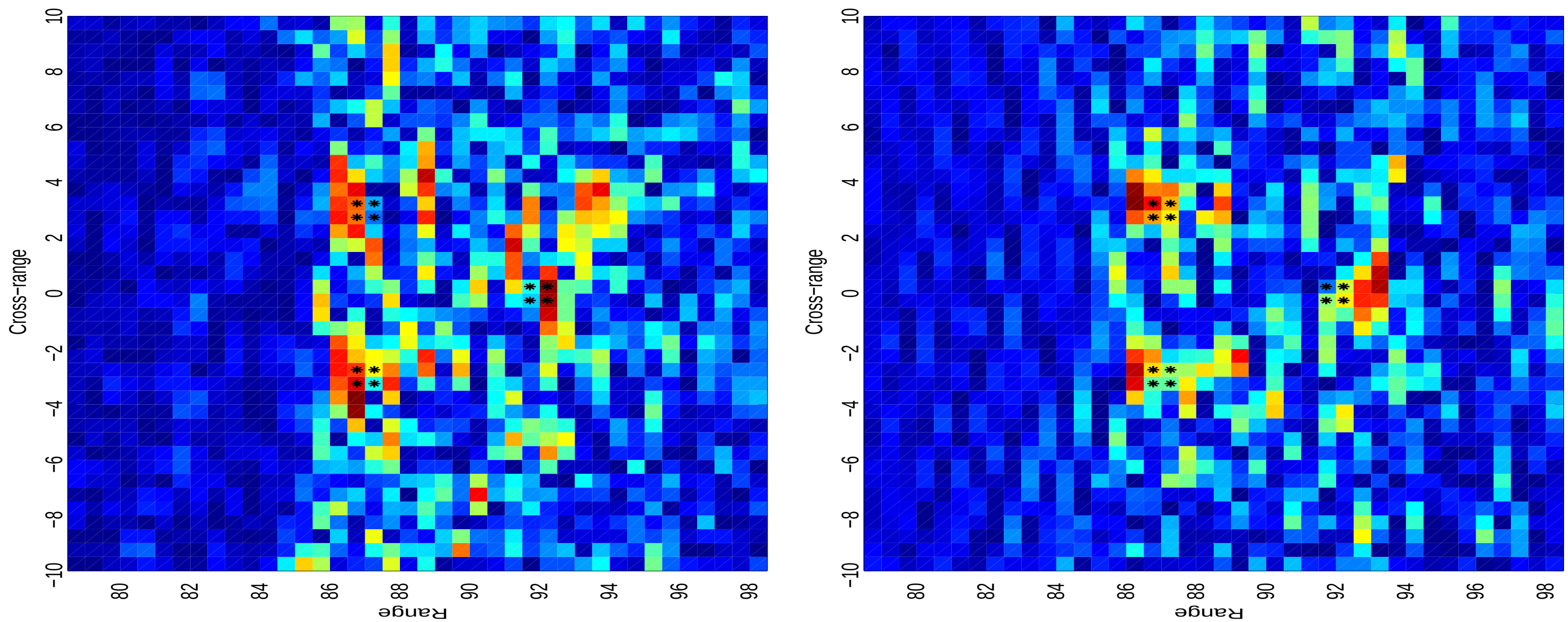

Coherent interferometry (CINT)

- we cross-correlate the traces locally in space and frequency:
  - cross-correlation in space is limitted by the decoherence length $X_d(\omega)$
    $$X_d(\omega) = \frac{c_0}{\omega \kappa_d}$$
  - cross-correlation in frequency is limitted by the decoherence frequency Ω_d
- CINT consists in migrating these cross-correlations to the search point $\vec{\mathbf{y}}^s$ using $G_c(\vec{\mathbf{x}}_s, \vec{\mathbf{y}}^s, \omega)$
- links with time reversal in RM (Bal, Ryzhik, Solna, Garnier, Papanicolaou)

CINT imaging functional

$$\mathcal{I}^{\text{CINT}}(\vec{\mathbf{y}}^s;\Omega_d,\kappa_d) = \int\int_{|\omega-\omega'|\le\Omega_d} d\omega d\omega' \sum_{\substack{r,r'=1\\ |\vec{\mathbf{x}}_r-\vec{\mathbf{x}}_{r'}|\le X_d\left(\frac{\omega+\omega'}{2}\right)}}^{N_r} \hat{P}(\vec{\mathbf{x}}_r,\vec{\mathbf{x}}_s,\omega)\overline{\hat{P}(\vec{\mathbf{x}}_{r'},\vec{\mathbf{x}}_s,\omega')}$$

$$\exp\{-i(\omega(\tau(\vec{\mathbf{x}}_r,\vec{\mathbf{y}}^s)+\tau(\vec{\mathbf{x}}_s,\vec{\mathbf{y}}^s))-\omega'(\tau(\vec{\mathbf{x}}_{r'},\vec{\mathbf{y}}^s)+\tau(\vec{\mathbf{x}}_s,\vec{\mathbf{y}}^s))\}$$

- when $\Omega_d = B$ and $X_d(\omega) = a$ (no smoothing) we obtain

$$\mathcal{I}^{\text{CINT}}(\vec{\mathbf{y}}^s;\Omega_d,\kappa_d) = \left[\mathcal{J}^{\text{KM}}(\vec{\mathbf{y}}^s)\right]^2$$

- CINT is a statistically stable smoothed migration method !
- Smoothing affects both range resolution c_0/Ω_d and cross range resolution $L\kappa_d \approx \lambda_0 L/X_d(\omega_0)$.

Adaptive CINT

- The parameters Ω_d and κ_d are estimated adaptively so as to achieve an optimal balance between statistical smoothing and resolution.

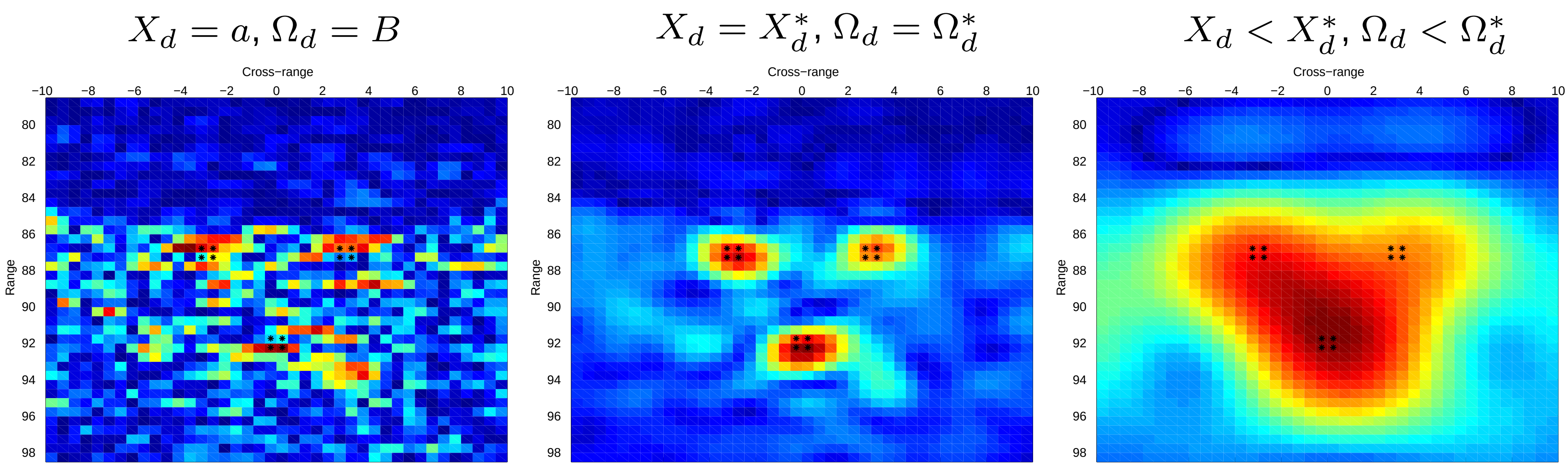

References

- L. Borcea, G. Papanicolaou and CT, Theory and applications of time reversal and interferometric imaging, Inverse Problems, vol 19, (2003), pp. 5139-5164.
- L. Borcea, G. Papanicolaou and CT, Interferometric array imaging in clutter, Inverse Problems, vol 21, (2005), pp. 1419-1460.
- L. Borcea, G. Papanicolaou and CT, Adaptive interferometric imaging in clutter and optimal illumination, Inverse Problems, vol. 22, (2006) pp. 1405-1436.
- L. Borcea, G. Papanicolaou and CT, Assymptotics for the space-time Wigner transform with applications to imaging, in Stochastic Differential Equations: Theory and Appliations. Volume in Honor of Professor Boris L. Rozovskii, edited by P.H. Baxendale and S.V. Lototsky, volume 2 of Interdisciplinary Mathematical Sciences, pp. 91–112 (World Scientific), 2007.

What happens in heavy clutter?

Computational domain and $v(z)$

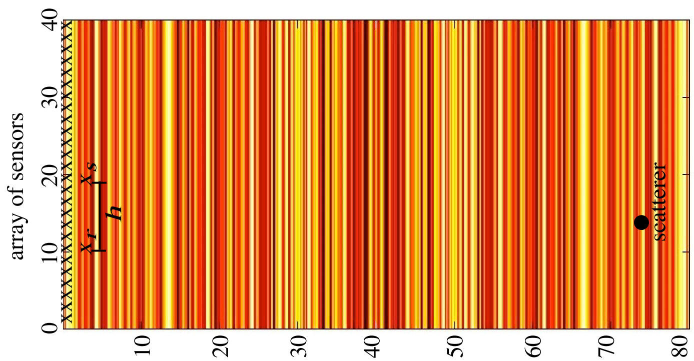

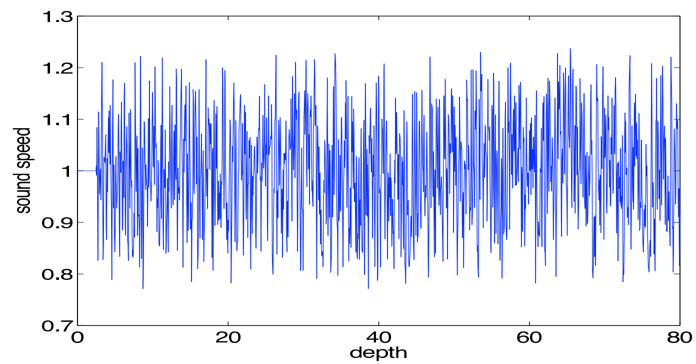

- Distance is scaled by λ_0. We have $f_0 = 10$Hz, $c_o = 1$Km/s, $\lambda_0 = 100$m, $B = [0, 25]$Hz.
- For the array $a = 40\lambda_0$, $N = 79$ transducers.
- For the rapid fluctuations $l = 0.02\lambda_0$, $\sigma = 0.08$.
- The scatterer is a disk of diameter λ_0 at depth $75\lambda_0$ and cross-range $15\lambda_0$.

What happens in heavy clutter?

Computational domain and $v(z)$

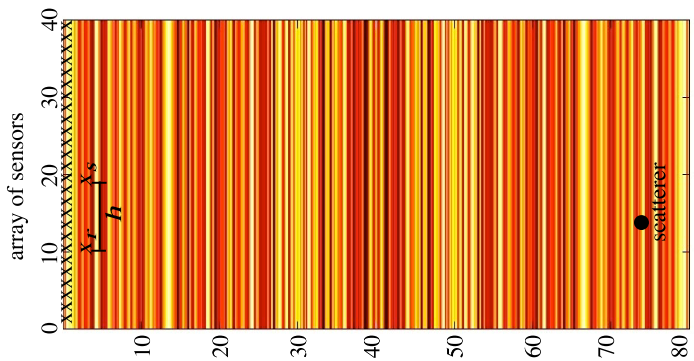

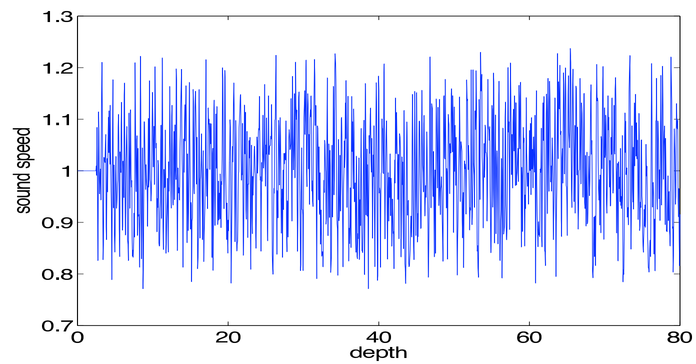

- The data is the $N \times N$ response matrix $\mathbb{P}(t)$, with $t \in [0,T]$ sampled on $N_t = 2^m$ points.

Imaging results

The data $P(t, \vec{\mathbf{x}}_r, \vec{\mathbf{x}}_s)$

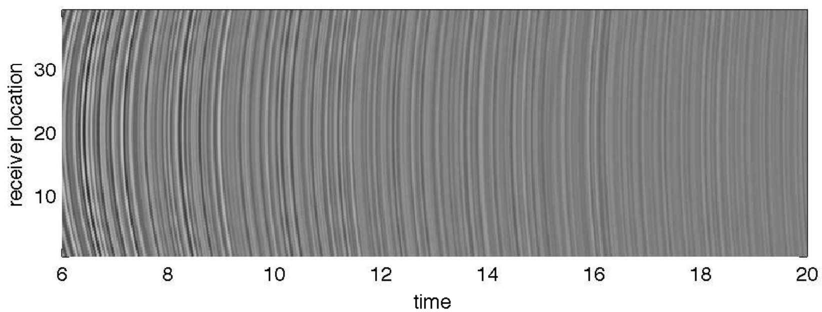

The image $\mathcal{J}^{\mathsf{KM}}(\vec{\mathbf{y}}^s)$

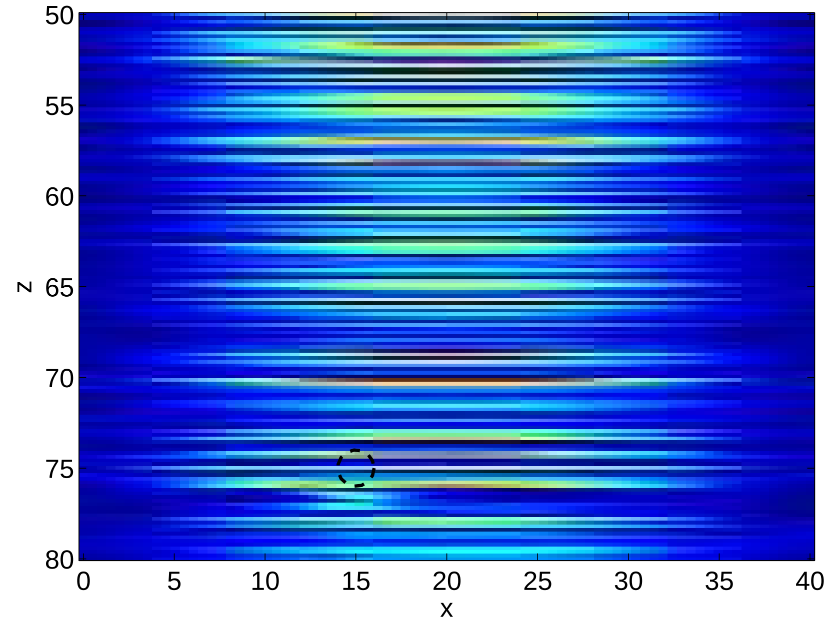

$$\mathcal{J}^{\mathsf{KM}}(\vec{\mathbf{y}}^s) = \sum_{\vec{\mathbf{x}}_s, \vec{\mathbf{x}}_r} \int d\omega \hat{P}(\vec{\mathbf{x}}_r, \vec{\mathbf{x}}_s, \omega) e^{-i\omega(\tau(\vec{\mathbf{x}}_s, \vec{\mathbf{y}}^s) + \tau(\vec{\mathbf{y}}^s, \vec{\mathbf{x}}_r))}$$

For $c(\vec{\mathbf{x}}) = c_0$ cst, $\tau(\vec{\mathbf{y}}, \vec{\mathbf{x}}) = \frac{|\vec{\mathbf{x}} - \vec{\mathbf{y}}|}{c_0}$

Note: we use here all sources on the array

Imaging results

The data $P(t, \vec{\mathbf{x}}_r, \vec{\mathbf{x}}_s)$

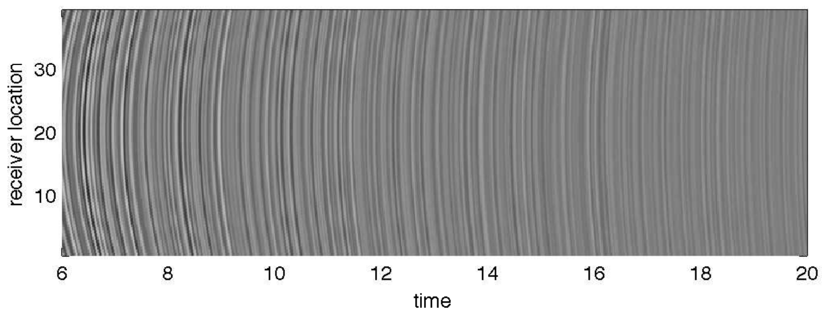

The image $\mathcal{I}^{\mathrm{CINT}}(\vec{\mathbf{y}}^s; \Omega_d, \kappa_d)$

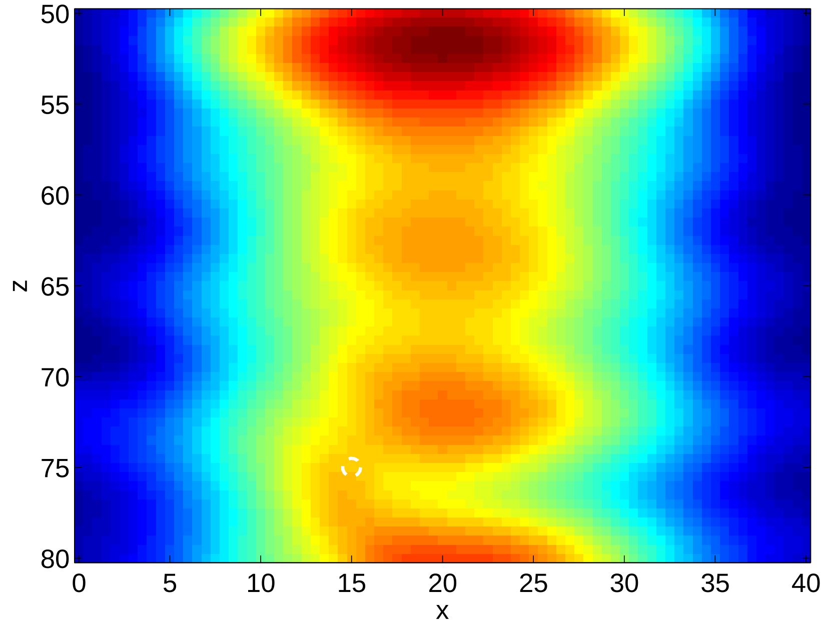

The idea

- Decompose the data in local time frequency windows and look at the behaviour of the singular values of these local matrices:

  the singular values correponding to pure clutter behave differently compared to the ones that correspond to coherent echoes

  ▷ build an algorithm for selecting the “part” in the data which corresponds to the coherend field scattered by the object we wish to image.

The algorithm I (LC in time)

- The Local Cosine (LC) transform of the data on a binary tree decomposes each trace $P_{rs}(t)$ to an orthonormal basis given by smooth windows χ modulated by cosine functions.

  $\forall$ level l in a binary tree, $0 \leq l \leq D$, define the segmentation: $t_j^l = j\Delta t_l = \frac{jT}{2^l}, \quad j = 0, 1, \ldots, 2^l - 1,$

The algorithm I (LC in time)

- The Local Cosine (LC) transform of the data on a binary tree decomposes each trace $P_{rs}(t)$ to an orthonormal basis given by smooth windows χ modulated by cosine functions.

  $\forall$ level l in a binary tree, $0 \le l \le D$, define the segmentation: $t_j^l = j\Delta t_l = \frac{jT}{2^l}, \quad j = 0, 1, \dots, 2^l - 1,$

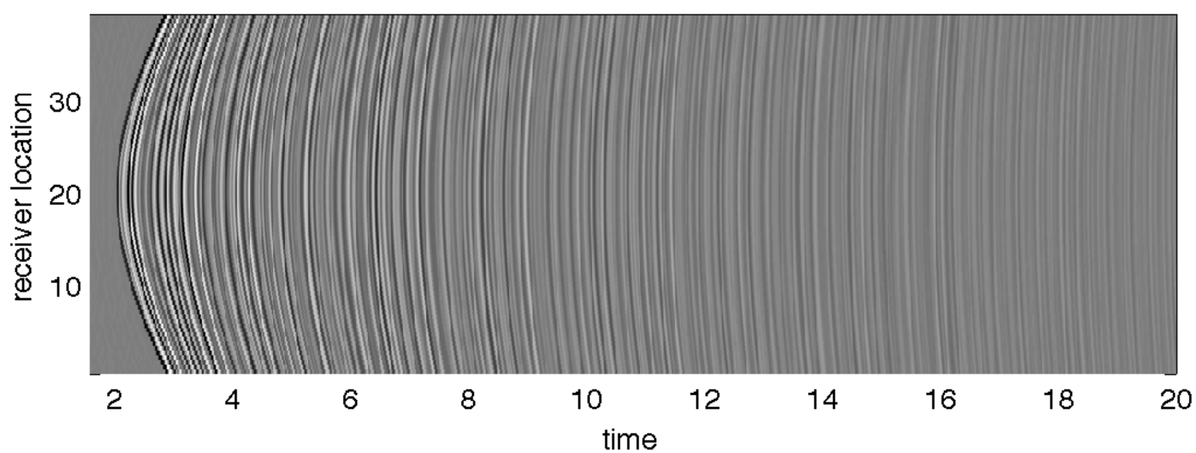

Level $l = 0$, 2^0 time window

The algorithm I (LC in time)

- The Local Cosine (LC) transform of the data on a binary tree decomposes each trace $P_{rs}(t)$ to an orthonormal basis given by smooth windows χ modulated by cosine functions.

  $\forall$ level l in a binary tree, $0 \leq l \leq D$, define the segmentation: $t_j^l = j\Delta t_l = \frac{jT}{2^l}, \quad j = 0, 1, \ldots, 2^l - 1,$

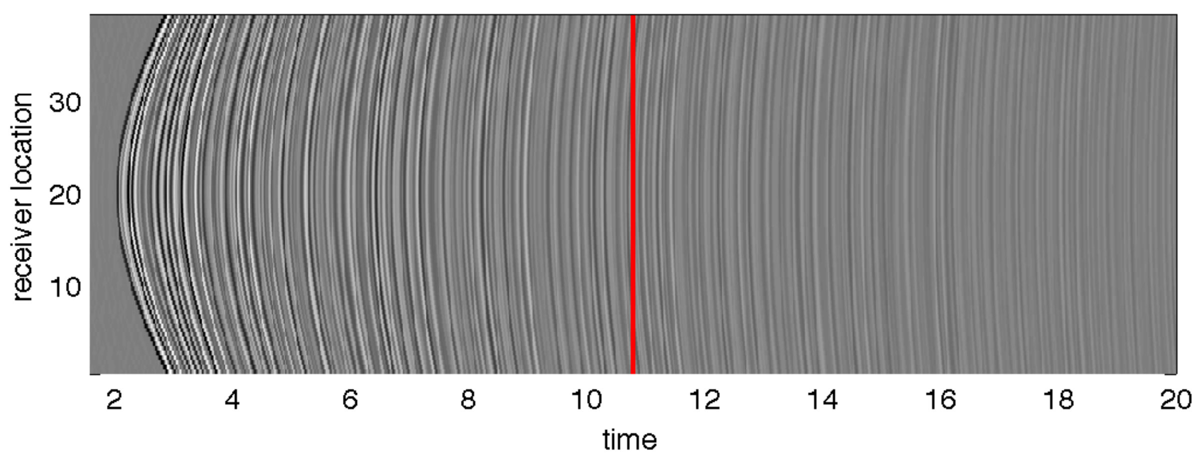

Level $l = 1$, 2^1 time windows $[0, \frac{T}{2}]$ and $[\frac{T}{2}, T]$

The algorithm I (LC in time)

- The Local Cosine (LC) transform of the data on a binary tree decomposes each trace $P_{rs}(t)$ to an orthonormal basis given by smooth windows χ modulated by cosine functions.

  $\forall$ level l in a binary tree, $0 \leq l \leq D$, define the segmentation: $t_j^l = j\Delta t_l = \frac{jT}{2^l}, \quad j = 0, 1, \ldots, 2^l - 1,$

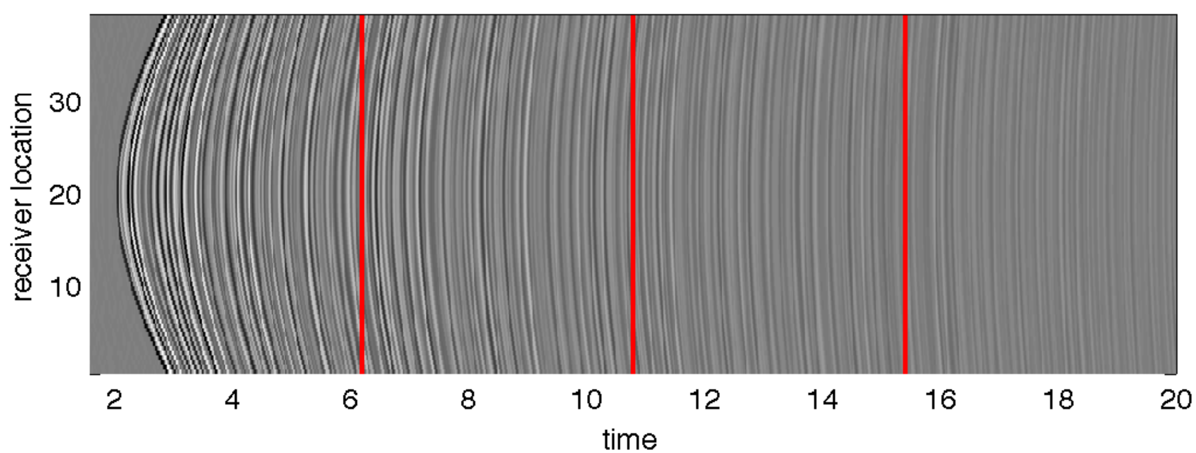

Level $l = 2$, 2^2 windows $[0, \frac{T}{4}]$, $[\frac{T}{4}, \frac{T}{2}]$, $[\frac{T}{2}, \frac{3T}{4}]$ and $[\frac{3T}{4}, T]$

The algorithm I (LC in time)

- The Local Cosine (LC) transform of the data on a binary tree decomposes each trace $P_{rs}(t)$ to an orthonormal basis given by smooth windows χ modulated by cosine functions.

  $\forall$ level l in a binary tree, $0 \leq l \leq D$, define the segmentation: $t_j^l = j\Delta t_l = \frac{jT}{2^l}, \quad j = 0, 1, \dots, 2^l - 1,$

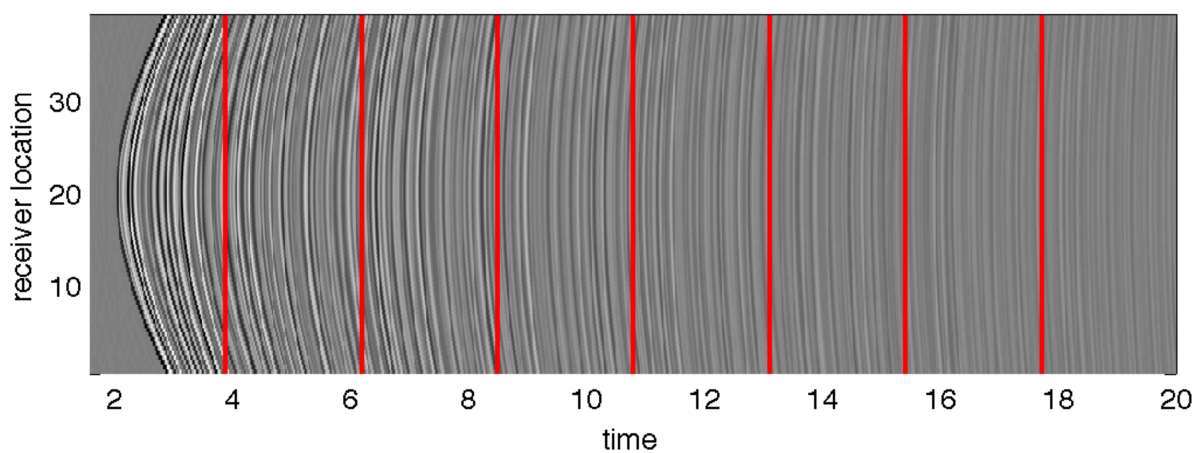

Level $l = 3$, 2^3 windows ....

The algorithm I (LC in time)

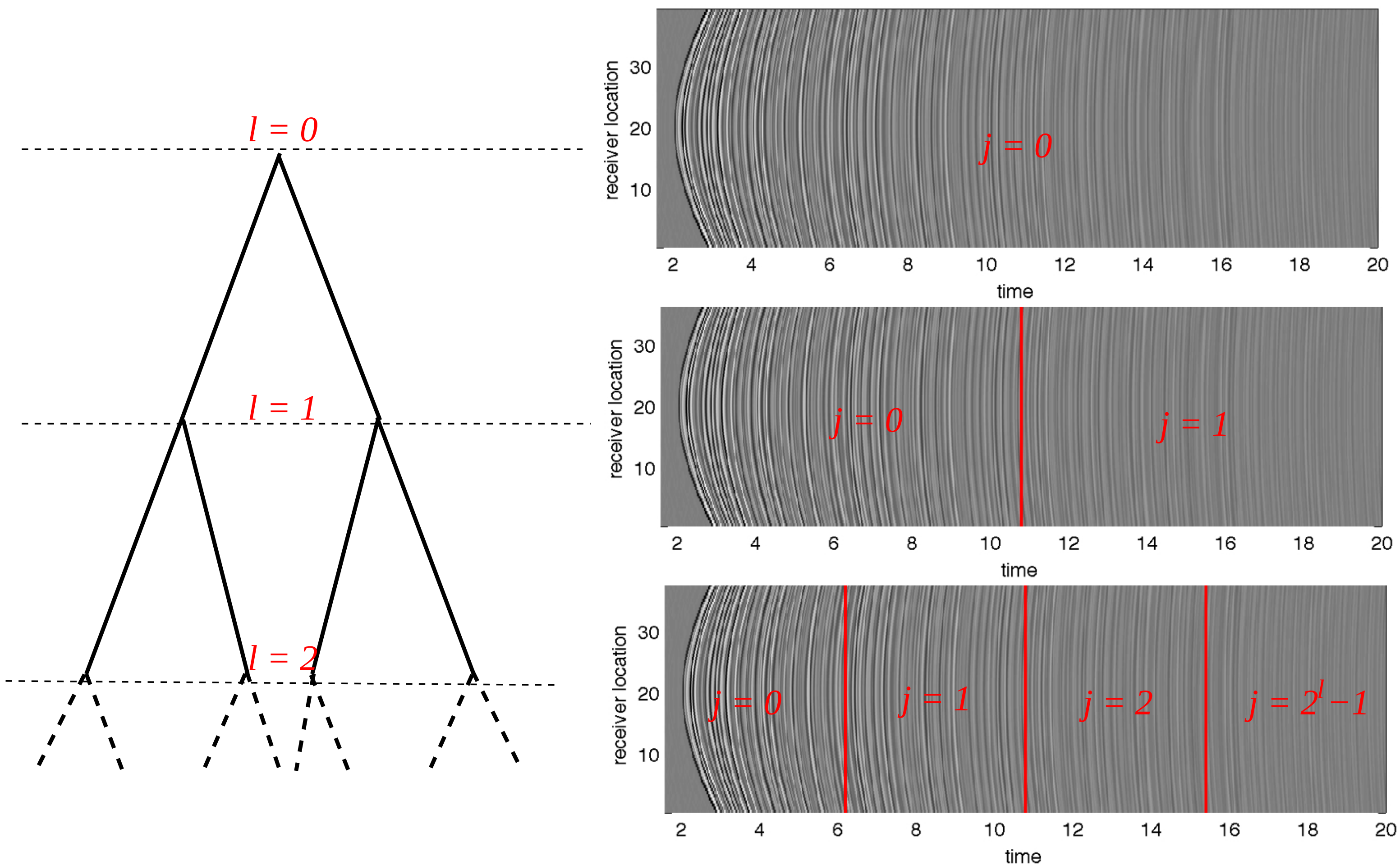

The algorithm I (LC in time)

- Each position j at level l is associated to the space :
$$\mathcal{F}_j^l = \left\{ \sqrt{\frac{2}{\Delta t_l}} \chi(\frac{t - t_j^l}{\Delta t_l}) \cos[\omega_n^l (t - t_j^l)] \right\}_{n \in \mathbb{N}}$$
with $\omega_n^l = \frac{\pi(n+1/2)}{\Delta t_l}$ the associated frequencies

  The union $\mathcal{F}_j^l$ over $j = 0, 1, \ldots, 2^l - 1$ gives an orthonormal basis of $L^2[0, T]$.

- The frequencies ω_n^l sample the *same* bandwidth $(0, \pi N_t / T)$, in steps $\pi / \Delta t_l$ that increase with l.

- at each node j at level l we have

$$\hat{\mathbb{P}}^l(t_j^l, \omega_n^l) = \left\{ \hat{P}^l(t_j^l, \omega_n^l, \vec{\mathbf{x}}_r, \vec{\mathbf{x}}_s) \right\}_{r,s=1,\ldots,N} .$$

The algorithm II (SVD)

- For each l and time window $j = 0, 1, \ldots 2^l - 1$ do the SVD of $\hat{\mathbb{P}}^l(t_j^l, \omega_n^l)$, frequency by frequency. Denote by $\sigma_q^{l,j}(\omega_n^l)$ the singular values, for $q = 1, \ldots N$.

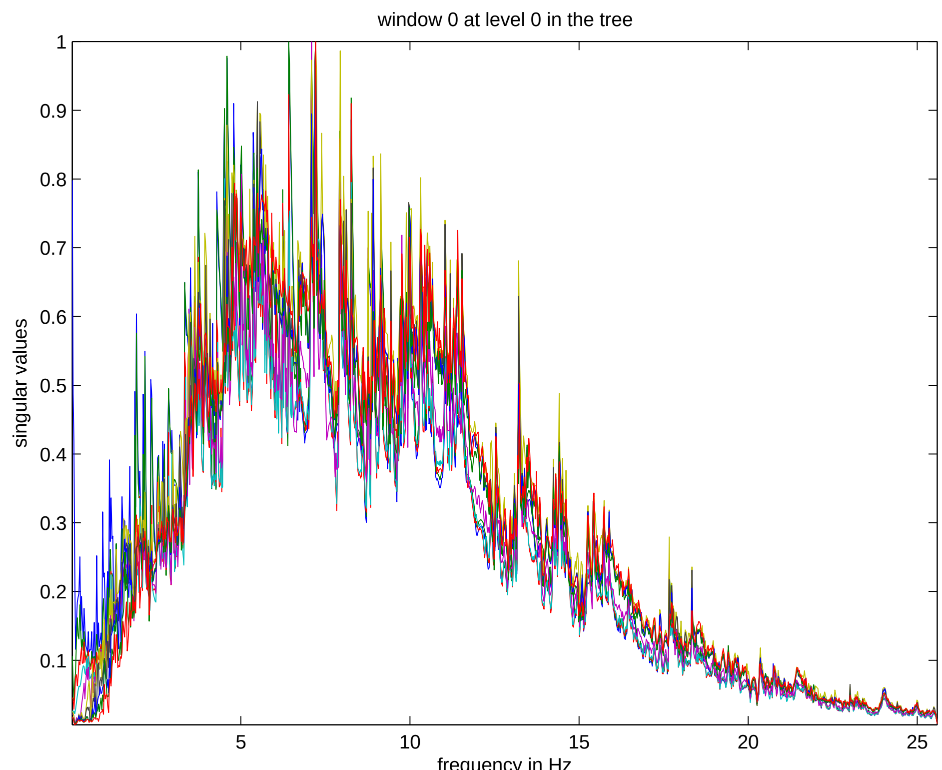

Normalized singular values $\tilde{\sigma}_q^{0,0}(\omega_n^0)$ vs frequency. We plot the first 10 of them.

The algorithm II (SVD)

$j = 0$ $j = 1$ $j = 2$ $j = 3$

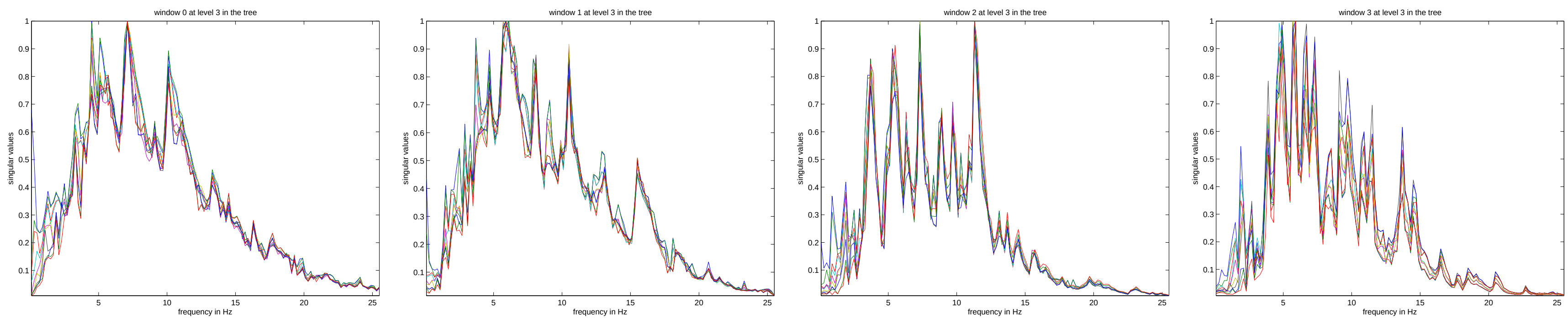

$j = 4$ $j = 5$ $j = 6$ $j = 7$

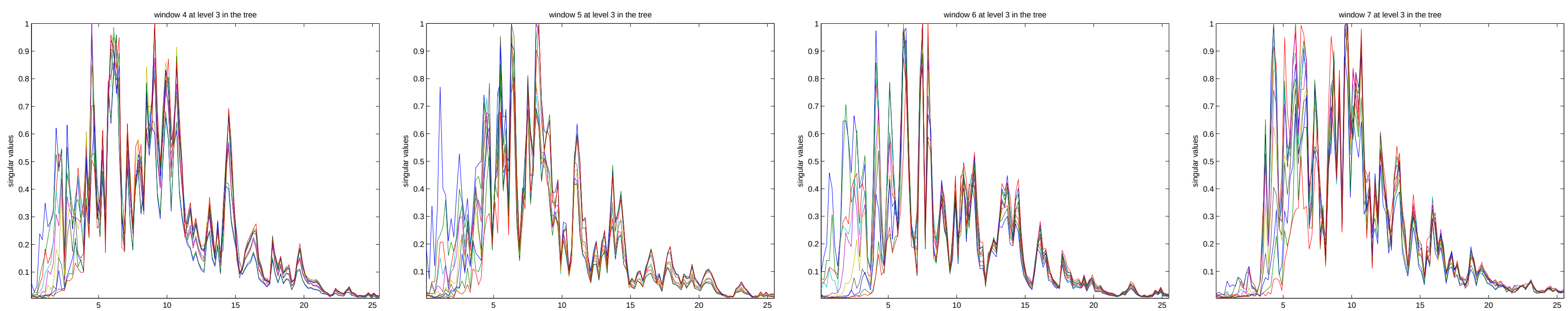

Normalized singular values $\tilde{\sigma}_q^{3,j}(\omega_n^3)$ vs. frequency. We plot the first 10 of them.

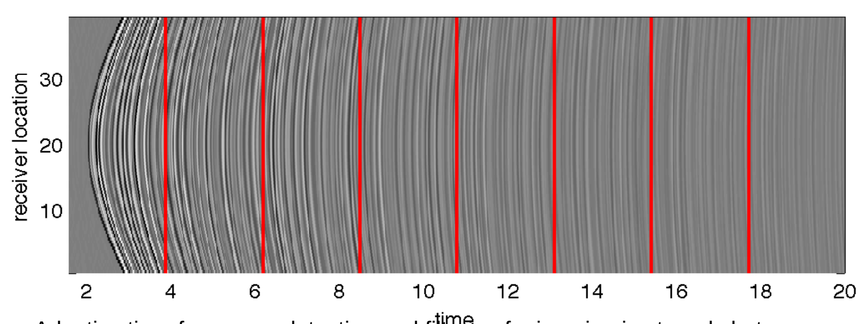

Good vs bad windows

$l = 3,\ j = 5$

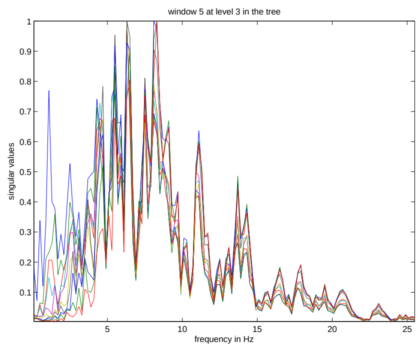

$l = 4,\ j = 11$

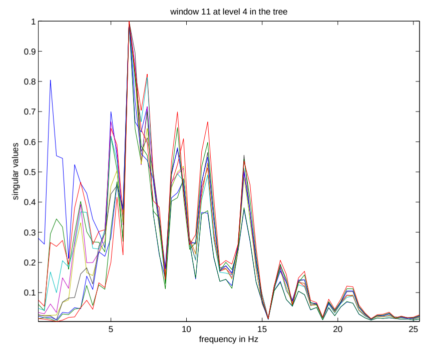

$l = 5,\ j = 23$

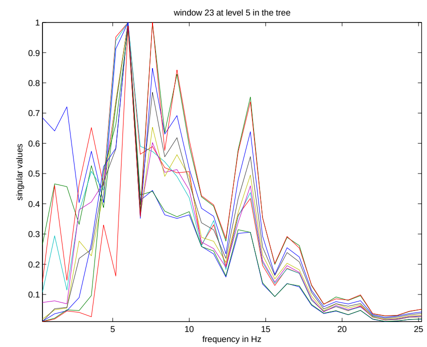

$l = 6,\ j = 47$

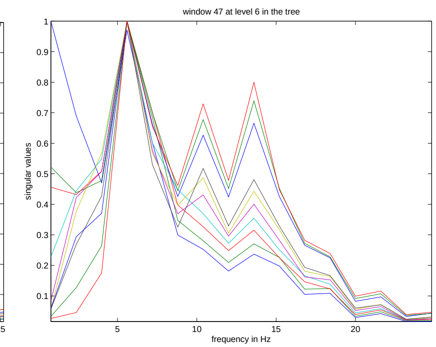

$l = 3, j = 2$

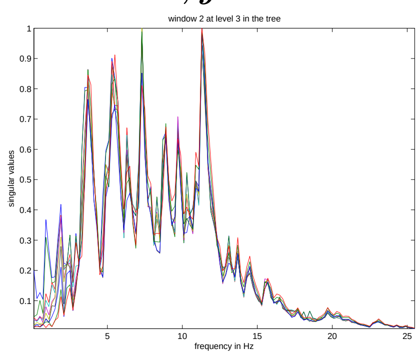

$l = 4, j = 5$

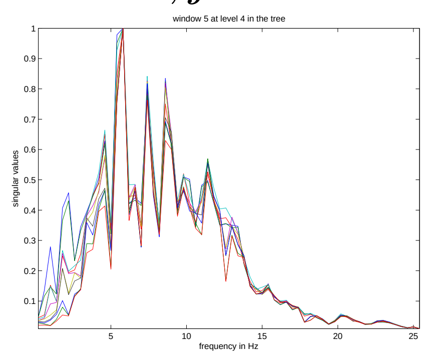

$l = 5, j = 11$

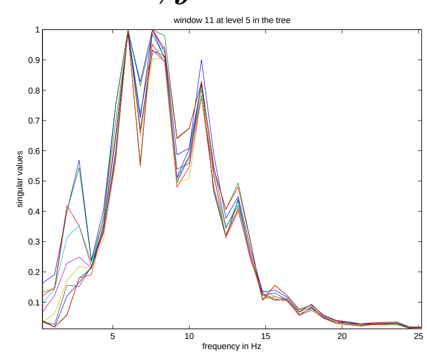

$l = 6, j = 23$

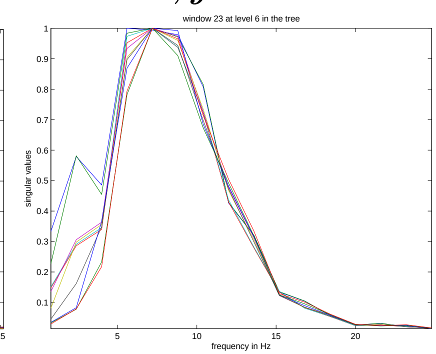

Top: The top 10 normalized singular values in the windows that contain the coherent echoes. Bottom: The top singular values in windows that contain pure clutter echoes.

The algorithm III (selection)

- Choose the frequency band $B \subseteq (0, \pi N_t/T)$ and the number Q of top singular values, to be used in the selection of the time windows, and the data filtering process.
- Form the matrices $\mathbb{S}^{l,j}$ of normalized singular values

$$\mathbb{S}^{l,j} = \left\{ \tilde{\sigma}_q^{l,j}(\omega_n^l) \right\}_{1 \le q \le Q,\, n \in \mathcal{N}^l}, \qquad \tilde{\sigma}_q^{l,j}(\omega_n^l) = \frac{\sigma_q^{l,j}(\omega_n^l)}{\max\limits_{n'} \sigma_q^{l,j}(\omega_{n'_l})}$$

over the badwidth B and select the widow of interest with a criterium based on the SVD of $\mathbb{S}^{l,j}$.

The algorithm III (selection)

- in the windows that contain pure clutter echoes the top singular values are clustered together: $\mathbb{S}^{l,j}$ are almost rank one.
- we expect a break in the pattern of the singular values in the windows that contain detectable coherent echoes: $\mathbb{S}^{l,j}$ has a significant second direction and the second singular value of $\mathbb{S}^{l,j}$ is large.

The algorithm III (selection)

- Let $\gamma_q^{l,j}$, for $1 \leq q \leq \min\{Q, |\mathcal{N}^l|\}$, be the singular values of $\mathbb{S}^{l,j}$. Our selection criterium at level l selects the window $j_\star^l$ at which

$$\lambda^{l,j} = \gamma_2^{l,j} / \gamma_1^{l,j},$$

  is maximal.
  At the next level $l+1$ we seek the maximum locally at the children of $j_\star^l$, if a clear maximum does not exist we stop at level l.

Results :the selection criterium

$l = 3,\ {\color{blue} j_\star^3} = 5$

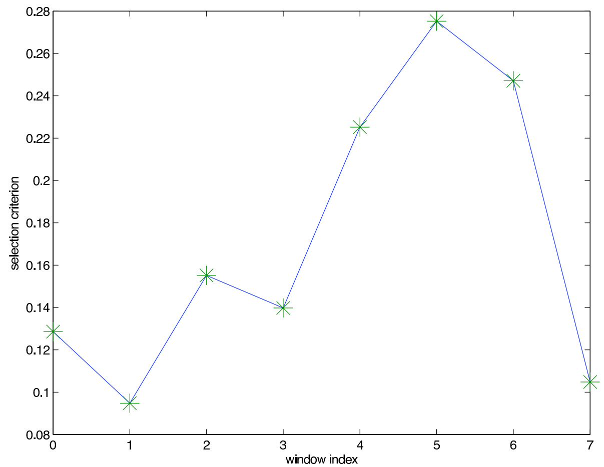

$l = 4,\ {\color{blue} j_\star^4} = 11$

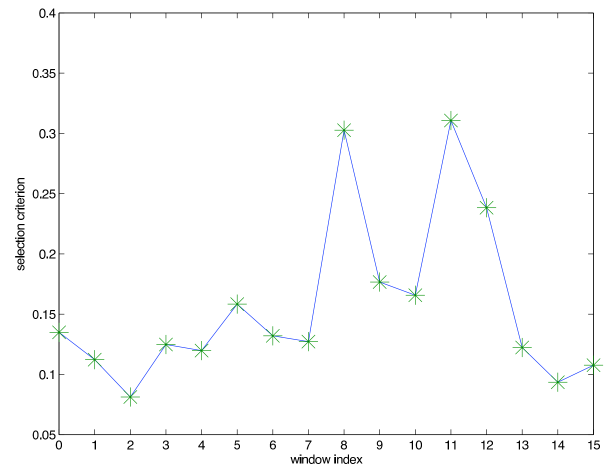

$l = 5,\ {\color{blue} j_\star^5} = 23$

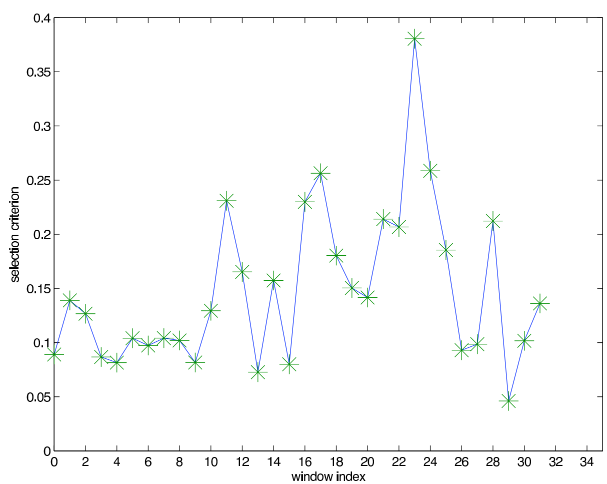

$l = 6,\ {\color{blue} j_\star^6} = 47$

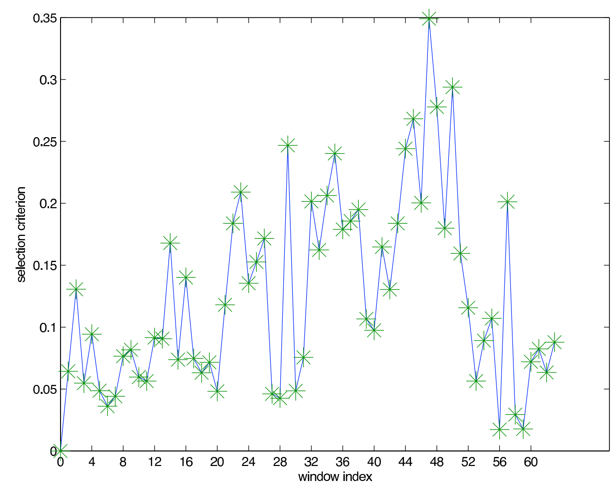

$\lambda^{l,j}$ as a function of the window index $j = 0, \dots, 2^l - 1$. $Q = 10$ and $B = [0, 5]$Hz.

The algorithm IV (filtering)

- In the selected time window, define the filter $\mathcal{F}^{j^l_\star}$ which sets to zero the LC coefficients in the windows that have not been selected, at level l,
  $\mathcal{F}^{j^l_\star}\hat{\mathbb{P}}^l(t^l_j, \omega^l_n) = 0$ for $j = 0, 1, \ldots, 2^l - 1, \quad j \neq j^l_\star$ and $n = 0, 1, \ldots N_t/2^l - 1.$
- Additional filtering is done by projecting $\hat{\mathbb{P}}^l(t_{j^l_\star}, \omega^l_n)$ on the space of low rank matrices with singular vectors corresponding to the “anomalous” top singular values for frequencies in B.

Results

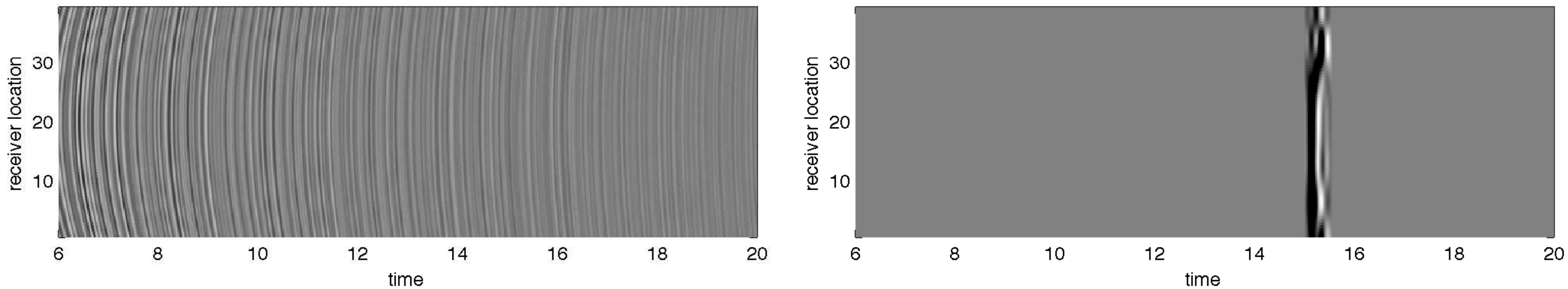

Central source. Left: initial traces. Right: final traces produced by the algorithm.

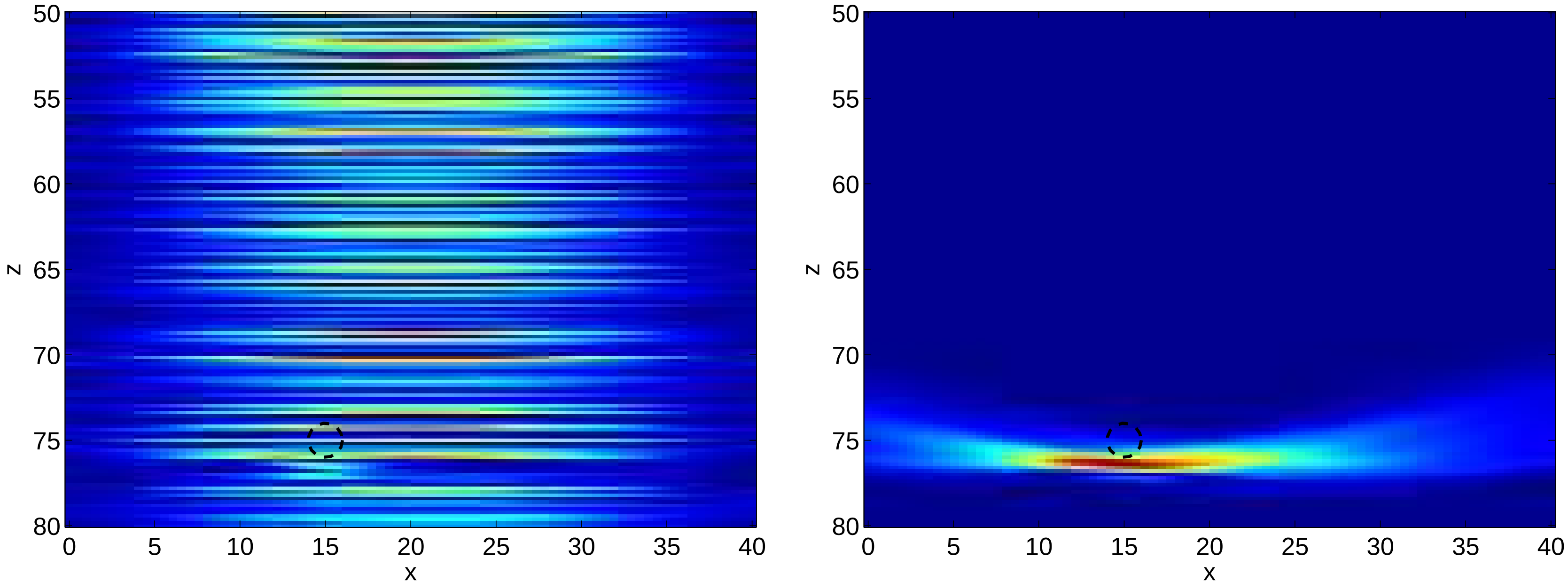

KM Left: initial image. Right: final image produced by the algorithm.

Results

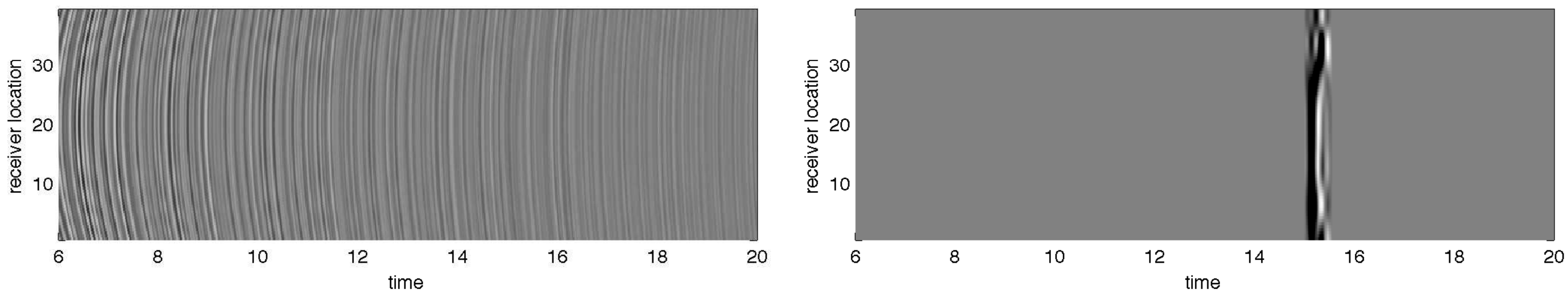

Central source. Left: initial traces. Right: final traces produced by the algorithm.

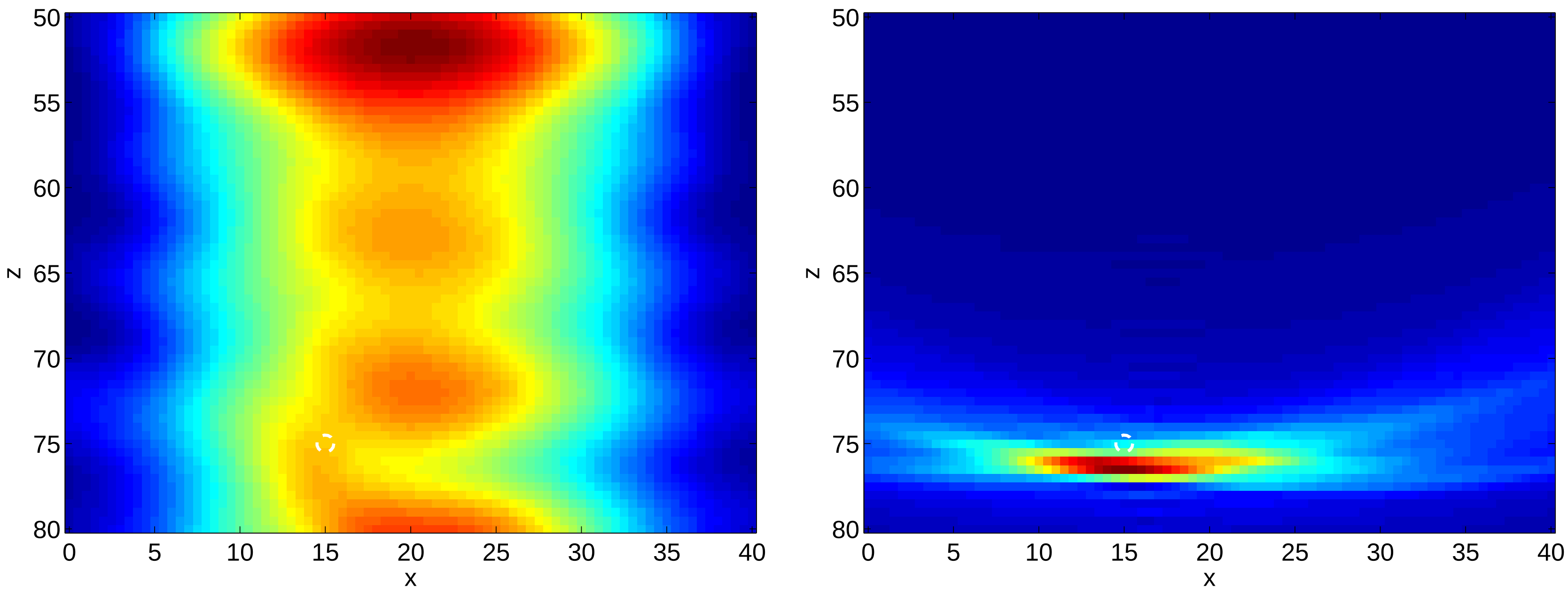

CINT Left: initial image. Right: final image produced by the algorithm.

Results

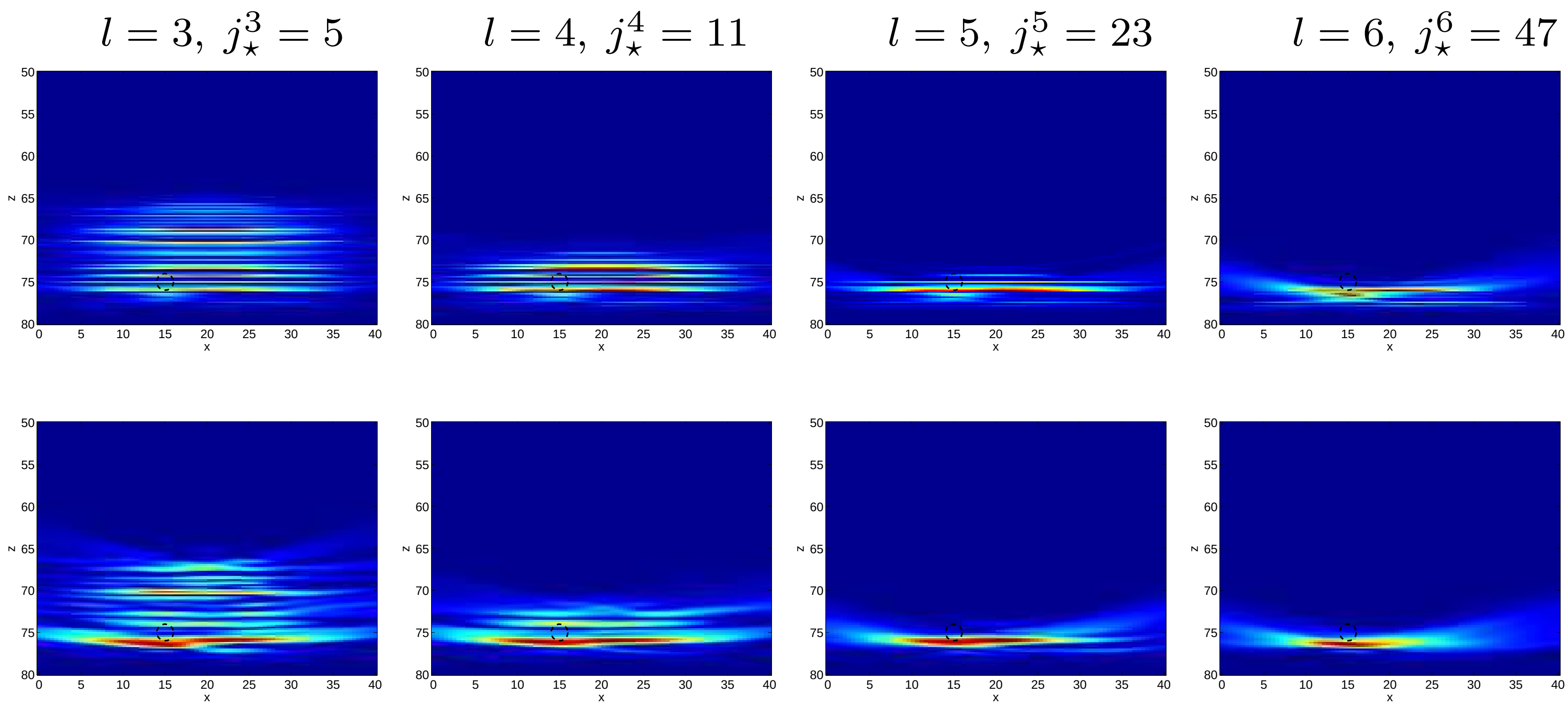

Top: no projection, Bottom: with projection. The scatterer is indicated with a black circle.

L. Borcea, G. Papanicolaou, C. T., *Data filtering for imaging in heavy clutter*, preprint, 2010.

R. Alonso, L. Borcea, G. Papanicolaou, C. T., *Detection and imaging instrongly backscattering randomly layered media*, Inverse Problems, vol. 27, (2011).

Results (combined)

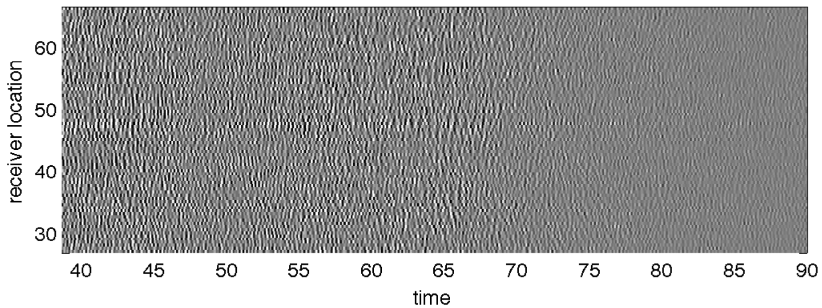

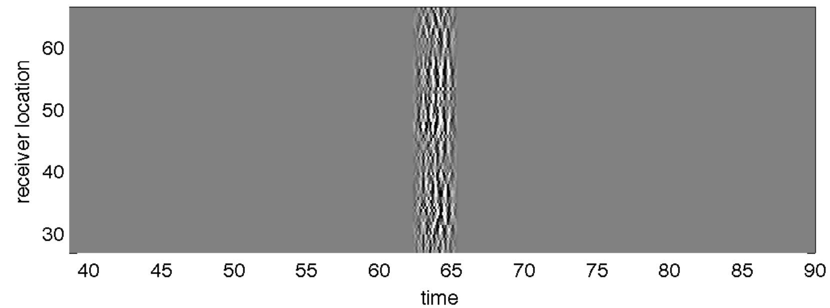

Central source. Left: initial traces. Right: final traces produced by the algorithm.

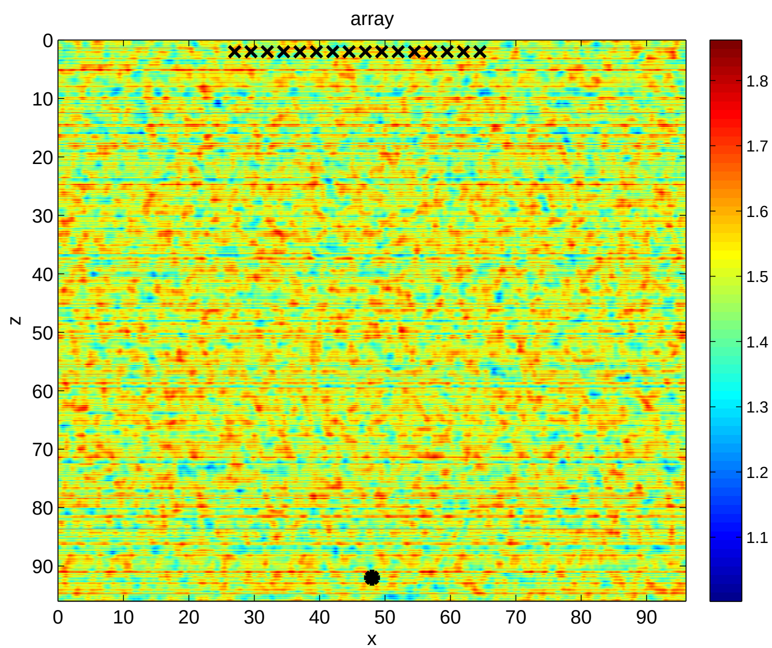

Results (combined)

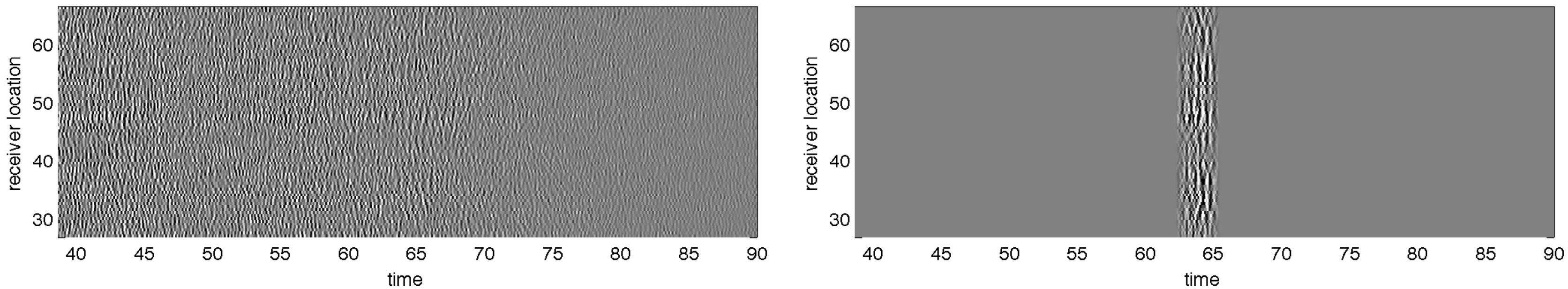

Central source. Left: initial traces. Right: final traces produced by the algorithm.

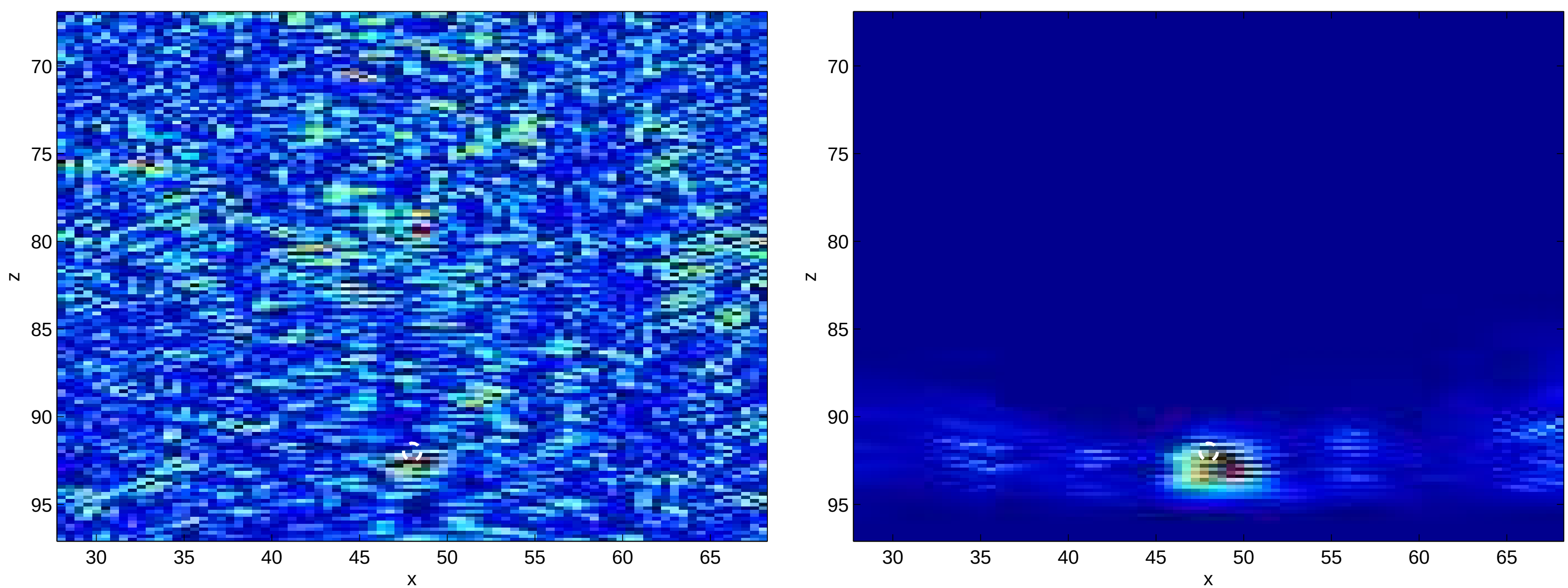

KM Left: initial image. Right: final image produced by the algorithm.

Results (combined)

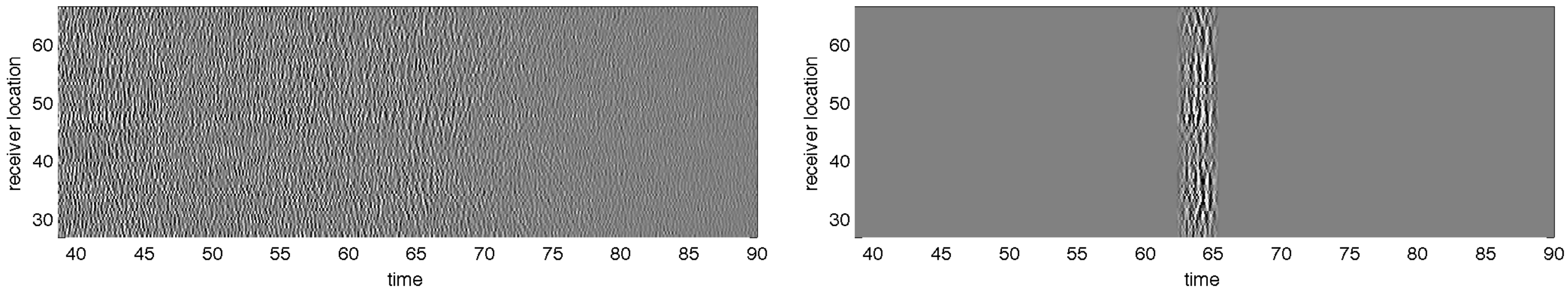

Central source. Left: initial traces. Right: final traces produced by the algorithm.

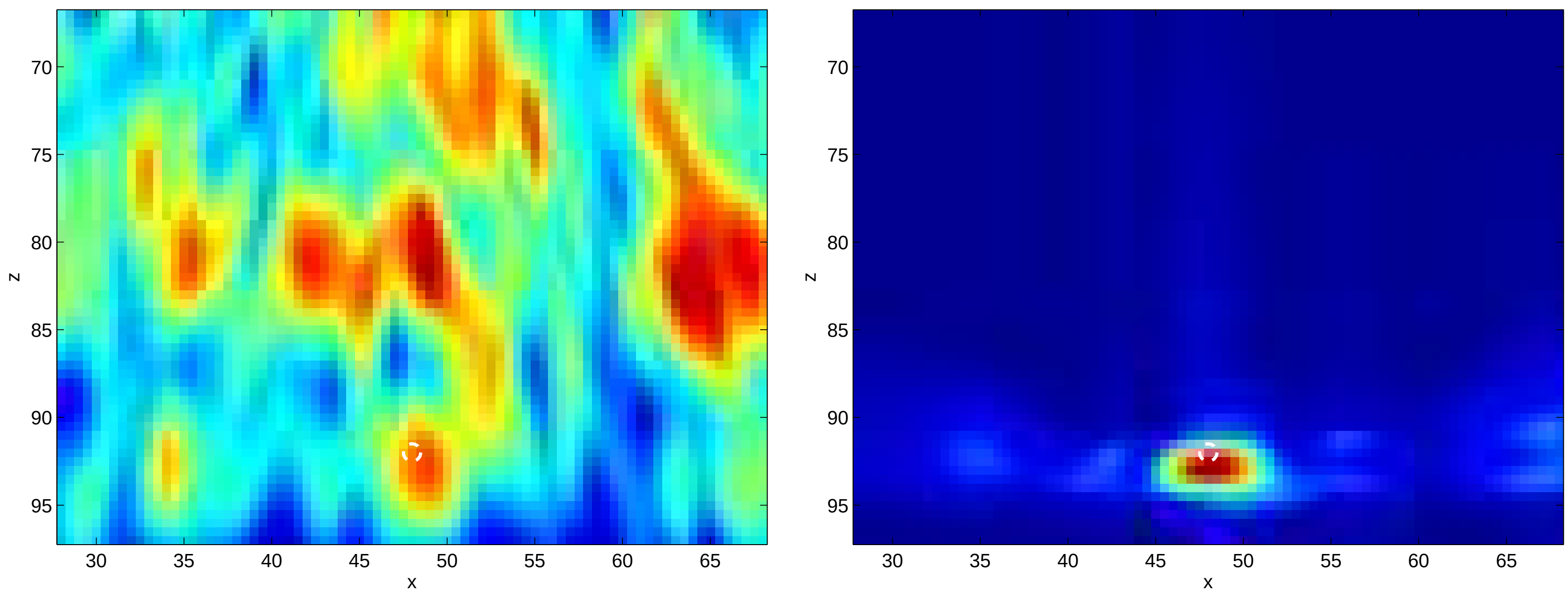

CINT Left: initial image. Right: final image produced by the algorithm.

Results (comparison)

combined

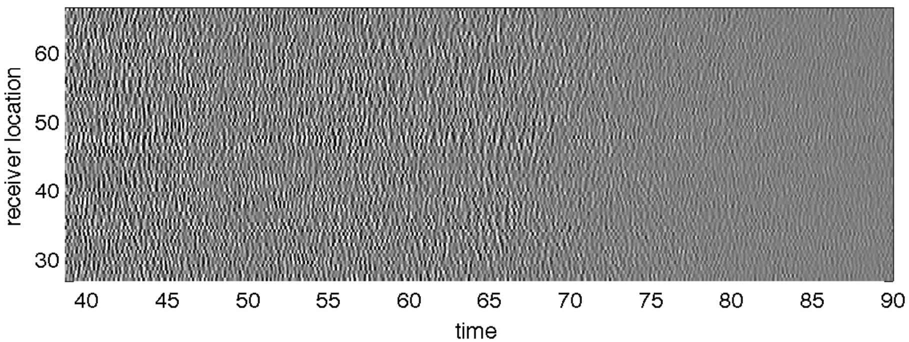

SNR$= -10$dB

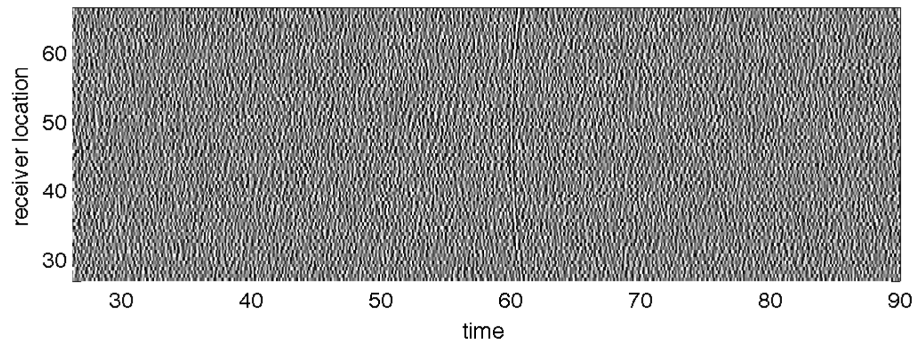

Results (comparison)

combined

SNR$= -10$dB

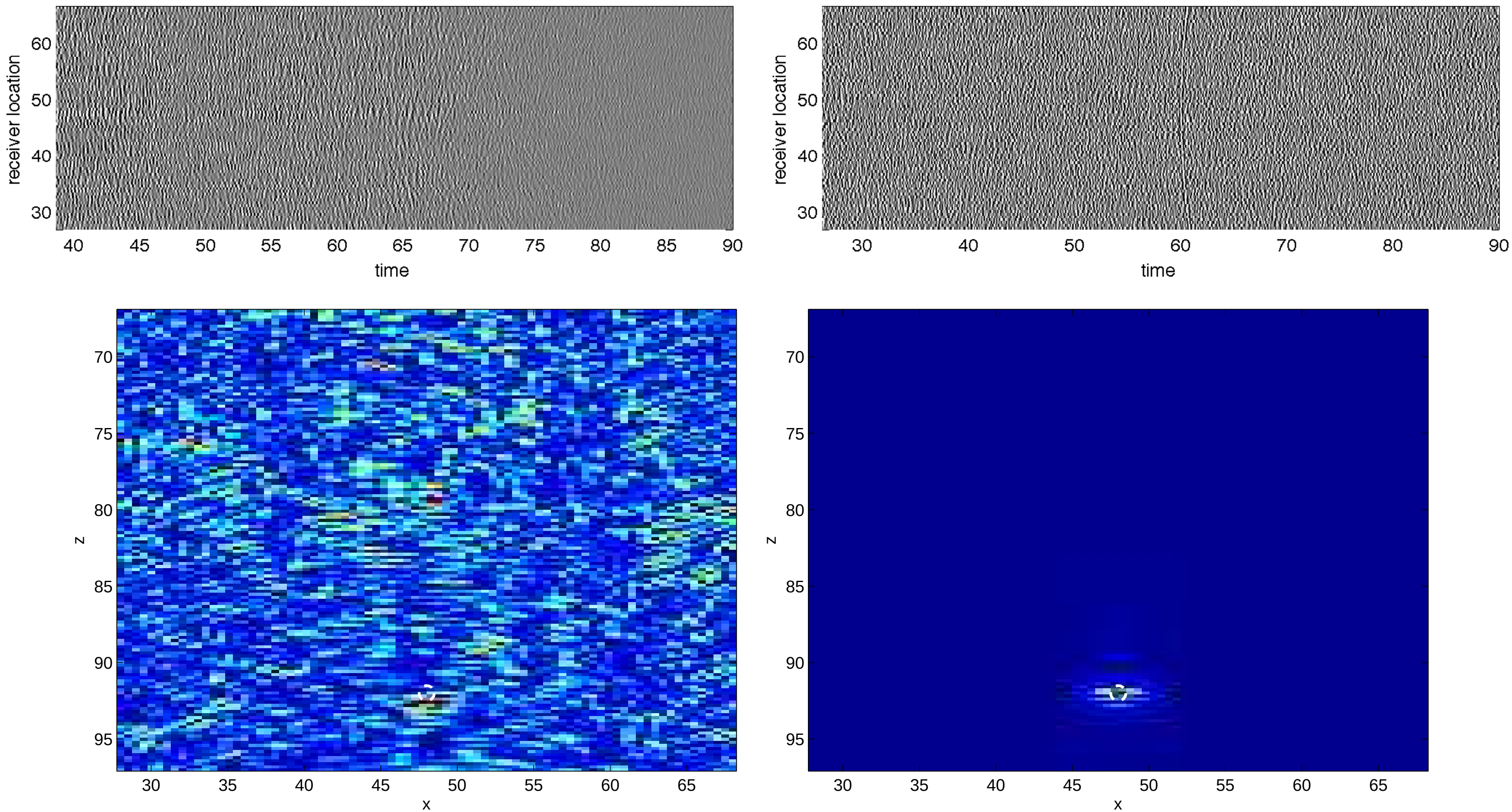

Conclusions

- The proposed filtering approach is general and does not use any *a priori* information on the clutter.
- We have analyzed theoretically the algorithm in the layered case and explained the behavior of the data: *clustering of the singular values for the clutter, detectability of coherent echoes only at lower frequencies*.
- needs to be tested for more general target configurations (multiple targets)
- when coherent imaging does not work $\rightarrow$ consider incoherent imaging methodologies that exploit some model to describe wave propagation in RM (cf. Bal & Pinaud, Borcea's talk)